WALKING TRAJECTORY GENERATION & CONTROL OF THE HUMANOID ROBOT SURALP

by
Evrim TAŞKIRAN

Submitted to the Graduate School of Engineering and Natural Sciences
in partial fulfillment of
the requirements for the degree of
Master of Science

Sabanci University
August 2009

WALKING TRAJECTORY GENERATION & CONTROL OF A HUMANOID ROBOT: SURALP

APPROVED BY:

Assist. Prof. Dr. Kemalettin ERBATUR (Thesis Advisor) .....

Prof. Dr. Asif SABANOVIC .....

Assoc. Prof. Dr. Mustafa ÜNEL .....

Assist. Prof. Dr. Ahmet Onat .....

Assist. Prof. Dr. Gürdal ERTEK .....

DATE OF APPROVAL: 10.08.2009

WALKING TRAJECTORY GENERATION & CONTROL
OF THE HUMANOID ROBOT: SURALP

Evrim TAŞKIRAN

ME, Master's Thesis, 2009

Thesis Supervisor: Assist. Prof. Dr. Kemalettin ERBATUR

Keywords: Bipedal Humanoid Robot, ZMP, Trajectory Generation, Online Balance Compensation, Walking Control

ABSTRACT

In recent years, the operational area of the robots started to extend and new functionalities are planned for them in our daily environments. As the human-robot interaction is being improved, the robots can provide support in elderly care, human assistance, rescue, hospital attendance and many other areas. With this motivation, an intensive research is focused around humanoid robotics in the last four decades.

However, due to the nonlinear dynamics of the robot and high number of degrees of freedom, the robust balance of the bipedal walk is a challenging task. Smooth trajectory generation and online compensation methods are necessary to achieve a stable walk.

In this thesis, Cartesian foot position references are generated as periodic functions with respect to a body-fixed coordinate frame. The online adjustment of these parameterized trajectories provides an opportunity in tuning the walking parameters without stopping the robot. The major contribution of this thesis in the context of trajectory generation is the smoothening of the foot trajectories and the introduction of ground push motion in the vertical direction. This pushing motion provided a dramatic improvement in the stability of the walking.

Even though smooth foot reference trajectories are generated using the parameter based functions, the realization of a dynamically stable walk and maintenance of the robot balance requires walking control algorithms. This thesis introduces various control techniques to cope with disturbances or unevenness of the walking environment and compensate the mismatches between the planned and the actual walking based on sensory feedback. Moreover, an automatic homing procedure is proposed for the adjustment of the initial posture before the walking experiments. The presented control algorithms include ZMP regulation, foot orientation control, trunk orientation control, foot pitch torque difference compensation, body pitch angle correction, ground impact compensation and early landing modification.

The effectiveness of the proposed trajectory generation and walking control algorithms is tested on the humanoid robot SURALP and a stable walk is achieved.

İNSANSI ROBOT SURALP'İN
YÜRÜME YÖRÜNGESİ SENTEZİ VE KONTROLÜ

Evrim TAŞKIRAN

ME, Master Tezi, 2009

Tez Danışmanı: Yrd. Doç. Dr. Kemalettin ERBATUR

ÖZET

Son yıllarda, robotların çalışma alanı genişlemekte ve günlük yaşamımızda belirli görevler almaları planlanmaktadır. İnsan-robot etkileşimi geliştikçe bu robotlar; hasta ve yaşlı bakımı, kurtarma gibi bir çok alanda hizmet verebileceklerdir. Bu yüzden, son kırk yıl içerisinde insansı robotlar konusunda yoğun bir araştırma yürütülmektedir.

Ancak, robotun doğrusal olmayan dinamiği ve yüksek sayıda serbestlik derecesi sebebi ile iki bacaklı yürümede dengeyi sağlamak oldukça zordur. Dolayısıyla, kararlı bir yürümeyi sağlamak için yumuşak bir yörünge oluşturulması ve çevrimiçi telafi yöntemleri gerekmektedir.

Bu tezde, Kartezyen ayak pozisyonu referansları, vücut kordinat ekseninde ifade edilmiş periyodik fonksiyonlar kullanılarak oluşturulmaktadır. Bu parametrik yörüngelerin çevrimiçi değiştirilmesi, yürüme parametrelerinin robotu durdurmadan ayarlanması gibi önemli bir olanak sunmaktadır. Yörünge sentezi kapsamında, bu tezin en önemli katkısı; ayak yörüngelerinin yumuşatılması ve dikey yönde zemin itme hareketinin önerilmesidir. Bu itme hareketi, yürümenin kararlılığında ciddi bir ilerleme sağlamıştır.

Parametre tabanlı fonksiyonlar kullanılarak yumuşak ayak referans yörüngeleri oluşturulsa bile, kararlı yürüyüşün sağlanması ve dengenin korunması için yürüme kontrol algoritmaları gerekmektedir. Bu tez, düz olmayan zemin koşullarına adapte olmak ve planlanan ve gerçek yürüyüş arasındaki farkları telafi etmek için sensör geri

beslemesine dayanan çeşitli kontrol teknikleri sunmaktadır. Bunlara ek olarak, yürüme deneylerinden önce robotun başlangıç duruşunu ayarlamak için otomatik bir sıfırlama prosedürü önerilmiştir. Sunulan kontrol algoritmaları; Sıfır Moment Noktası ayarlama kontrolü, ayak yönelim kontrolü, vücut yönelim kontrolü, ayak yunuslama moment farkı telafisi, vücut yunuslama açısı iyileştirmesi, zemin darbe telafisi ve erken basma referans iyileştirmesini içermektedir.

Önerilen yörünge sentezi ve yürüme kontrol algoritmalarının etkililiği insansı robot SURALP üzerinde denenmiş ve kararlı bir yürüyüş başarılmıştır.

To my beloved family

ACKNOWLEDGEMENTS

It is difficult to express my gratitude to my MS. supervisor, Assist. Prof. Dr. Kemalettin ERBATUR for his great effort and academic guidance on this work. He made this thesis possible by his encouragement, enthusiasm, inspiration and patience in teaching during my thesis study and all Master education. I feel myself privileged as his Master student.

I would like to express my greatest appreciation to Assoc. Prof. Dr. Mustafa ÜNEL for his invaluable support and sharing of brilliant ideas on vision based control.

I am grateful to my thesis committee members Mustafa ÜNEL, Asif SABANOVIC, Ahmet ONAT and Gürdal ERTEK for their valuable review and comments on the thesis.

I would like to acknowledge the financial support provided by TÜBİTAK through the project "Two Legged Humanoid Robot Design, Construction and Control" under the grant 106E040 and TÜBİTAK BIDEB scholarship.

I would sincerely thank to the SURALP team, particularly Utku Seven, Özer Koca and Metin Yılmaz for their valuable friendship, motivational support and team cooperation during my Master study.

I am indebted to all my friends, especially Kaan Öner, Can Berk Güder, Ozan Mutluer, Ahmet Yasin Yazıcıoğlu, Berk Çallı, Ahmetcan Erdoğan, Aykut Cihan Satıcı, Hakan Kapson, Yeşim Hümay Esin, Emrah Deniz Kunt and many other members of the Mechatronics Graduate Laboratory.

Finally and most importantly, my greatest thanks go to my parents, Neşe Taşkıran and Neşet Taşkıran and my brother Evren Taşkıran for all their eternal love, support and trust. Without them, it would not be possible to reach my academic achievements throughout my life. To them I dedicate this thesis.

WALKING TRAJECTORY GENERATION & CONTROL
OF THE HUMANOID ROBOT SURALP

TABLE OF CONTENTS

LIST OF FIGURES

LIST OF TABLES

LIST OF SYMBOLS

T_{step}	:	Step period
T_{ssp}	:	Single support period
T_{dsp}	:	Double support period
T_{push}	:	Ground push period
T_{delay}	:	Swing delay period
l_{right}	:	Effective length of the right leg
l_{left}	:	Effective length of the left leg
d_{step}	:	Step size
x_{ref}	:	x direction foot reference
y_{ref}	:	y direction foot reference
z_{ref}	:	z direction foot reference
$x_{ref\ asymmetry}$	:	x reference asymmetry
$y_{ref\ asymmetry}$	:	y reference asymmetry
d_{swing}	:	Swing amplitude
$d_{swing\ offset}$	:	Swing offset
h_{push}	:	Ground push amplitude
h_{height}	:	Step height
K_p	:	Proportional control gain
K_i	:	Integral control gain
K_d	:	Derivative control gain
x_{ZMP}	:	Zero Moment Point in x-direction
y_{ZMP}	:	Zero Moment Point in y-direction

ϑ_{roll}	:	Ankle joint roll angle
$\vartheta_{trunk\ roll}$	:	Trunk roll angle
K_{roll}	:	Foot roll orientation low pass filter gain
λ_{roll}	:	Foot roll orientation low pass filter time constant
ϑ_{pitch}	:	Ankle joint pitch angle
$\vartheta_{trunk\ pitch}$	:	Trunk pitch angle
T_{pitch}	:	Ankle joint pitch torque
F_z	:	Ground reaction force in z direction
m_l	:	Mass coefficient of the desired mechanical admittance
b_l	:	Damping coefficient of the desired mechanical admittance
k_l	:	Stiffness coefficient of the desired mechanical admittance

LIST OF ABBREVIATIONS

ZMP	:	Zero Moment Point
PID	:	Proportional Integral
2-D	:	Two Dimensional
3-D	:	Three Dimensional
LIPM	:	Linear Inverted Pendulum Mode
D.O.F	:	Degrees of Freedom
COG	:	Center of Gravity
COM	:	Center of Mass
DH	:	Denavit Hartenberg
HD	:	Harmonic Drive
CPG	:	Central Pattern Generator
F/T	:	Force / Torque
FSR	:	Force Sensing Resistor
SSP	:	Single Support Phase
DSP	:	Double Support Phase

Chapter 1

1. INTRODUCTION

Robots have been playing a significant role as automation devices in industrial environments. In recent years, their operational area started to extend and new functionalities are planned for them in our daily environments, like hospitals, offices and homes. As the human-robot interaction is being improved, the robots can provide locomotion and manipulation support to people, such as elderly care, human assistance, rescue, hospital attendance and many others. With this motivation, an intensive research is focused around humanoid robotics in the last four decades.

One of the major reasons of the interest in humanoid robotics is the adaptability to human environment due to the anthropomorphic structure of bipedal robots. So, they can avoid obstacles and function properly in human environments like humans do. Furthermore, humanoid robots can operate a variety of difficult and hazardous tasks in rough work environments as a result of the capability of performing human actions, such as fire rescue, radioactive environments and space applications.

However, due to the nonlinear dynamics of the robot and high number of degrees of freedom, the robust balance of the bipedal walk is a challenging task. Many studies on humanoid robotics are focused around humanoid robot walking control in the last decades.

In addition to achieving a stable bipedal walk on flat surfaces, it is also important to keep the robot stable during walking on an unstructured environment. Since one of the major objectives of humanoid robotics research is the adaptation of the humanoid robots to human environment, the stability of the humanoid robot must be maintained during walking on uneven or inclined planes, which are very typical ground conditions encountered in human daily life. Furthermore, the robot should move

robustly during the interaction with the environment, such as manipulation tasks and human-robot interaction.

Smooth trajectory generation and online compensation methods are necessary to achieve a stable walk. Many different approaches in reference generation and control techniques on the bipedal walking are presented in the humanoid robotics literature. The contribution of this thesis is both on trajectory generation and walking control algorithms.

In this thesis, the reference trajectories are generated as periodic functions of the Cartesian position references for coordinate frame centers attached to the two feet, with respect to a coordinate frame attached to the trunk of the biped robot. The joint trajectories are computed using the inverse kinematics, based on these reference positions of the feet.

The mathematical functions used in the generation of foot trajectories are easy to compute and this trajectory generation method enables the smoothing of these trajectories at specific instants of the walk. Furthermore, the online adjustment of these parameterized trajectories is possible and this flexibility of changing all the variables online provides an important opportunity in tuning the walking parameters without stopping the robot.

The major contribution of this thesis in the context of trajectory generation is the smoothening of the foot trajectories and the introduction of ground push motion of the feet in z-direction. This pushing motion provided a dramatic improvement in the stability of the walking.

Even though smooth foot reference trajectories are generated using the parameter based functions, the realization of a dynamically stable walk and maintenance of the robot balance requires walking control algorithms. This thesis introduces various control techniques to cope with disturbances or unevenness of the walking environment and compensate the mismatches between the planned and the actual walking based on sensory feedback from force/torque sensors at the ankles and an inclinometer mounted on the robot torso. The control methods proposed in the thesis modify the walking trajectory generation or directly act to the computed joint references. Moreover, an automatic homing procedure is proposed for the adjustment of the initial posture before the walking experiments. The presented control algorithms include ZMP regulation, foot orientation control, trunk orientation control, foot pitch

torque difference compensation, body pitch angle correction, ground impact compensation and early landing modification.

The walking experiments are carried out on the humanoid robot platform: SURALP (**S**abanci **U**niversity **R**obotics Rese**A**rch **L**aboratory **P**latform), which is designed in Sabanci University in the framework of a project funded by TUBITAK (The Scientific and Technological Research Council of Turkey). The effectiveness of the generated reference trajectories and the presented online compensation algorithms is tested on SURALP and a stable walk is achieved.

The rest of the thesis is organized as follows. Chapter 2 presents a brief history of the humanoid robots in the world, the terminology used in bipedal locomotion and a literature survey on reference generation methods and walking balance control algorithms. Chapter 3 presents the bipedal humanoid robot model, the sensory system and the controller hardware structure. The reference trajectory generation method used throughout this thesis is introduced in Chapter 4. Chapter 5 describes balance control algorithms applied during the homing process and biped walking. Experimental walking results and performances of the employed control algorithms are discussed in Chapter 6. Finally, the conclusions and future works are presented in Chapter 7.

Chapter 2

2. LITERATURE REVIEW

2.1. Examples of Humanoid Robots

In late 1960's interest of researchers on humanoid robotics increased and many experimental robots started to be developed. During these years, Professor Ichiro Kato who pioneered robotic studies in Japan started studying human locomotion and in 1967 constructed an artificial lower-limb biped walker WL-1 in Waseda University [1]. With this fundamental design, basic analysis of bipedal locomotion started (Figure 2.1). After other prototypes WL-3 and WL-5, in 1973 world's first full-scale anthropomorphic robot; WABOT-1 is constructed. This robot was able to walk statically, change direction while walking and interact with the environment like measuring the distance and communicating with human in Japanese with artificial external receptors. After studies on the realization of quasi-dynamic walking with WL-9DR and plane walking with WL-10R, in 1984 by Takanishi et al. first dynamic walking is succeeded with the WL-10RD prototype, which used torque feedback from the torque sensors attached to the ankle and hip joints [2]. These studies continued with the hydraulic biped robot family WL-12 and still continue with parallel mechanism prototypes WL-15 and WL-16.

With the aim of creating a human-size robot, which is actuated by electric motors and has the same walking speed with human, WABIAN (**WA**seda **BI**ped Hum**AN**oid robot) was created in 1996 consisting 35 D.O.F. As studies on robot-environment interaction are conducted with this prototype, in 1999 WABIAN-RII is introduced, which was able to follow human motions by the parameterization of body motions [3]. After the prototype WABIAN-RIII created to absorb impact during landing of the foot, in 2004 WABIAN-RIV is presented, which is able to mimic some abilities

of human senses with the help of its vision and voice recognition system. WABIAN-RIV has 43 D.O.F., a 1.89 m height and 127 kg weight (Figure 2.2).

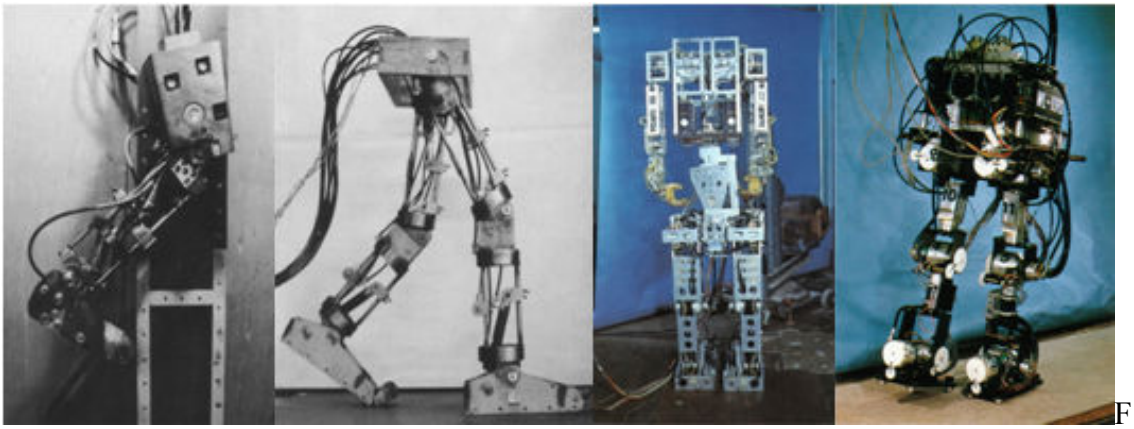

Figure 2.1 First examples of humanoid robots from Waseda University: WL-1, WL-3, WABOT-1 and WL-10RD (from left to right)

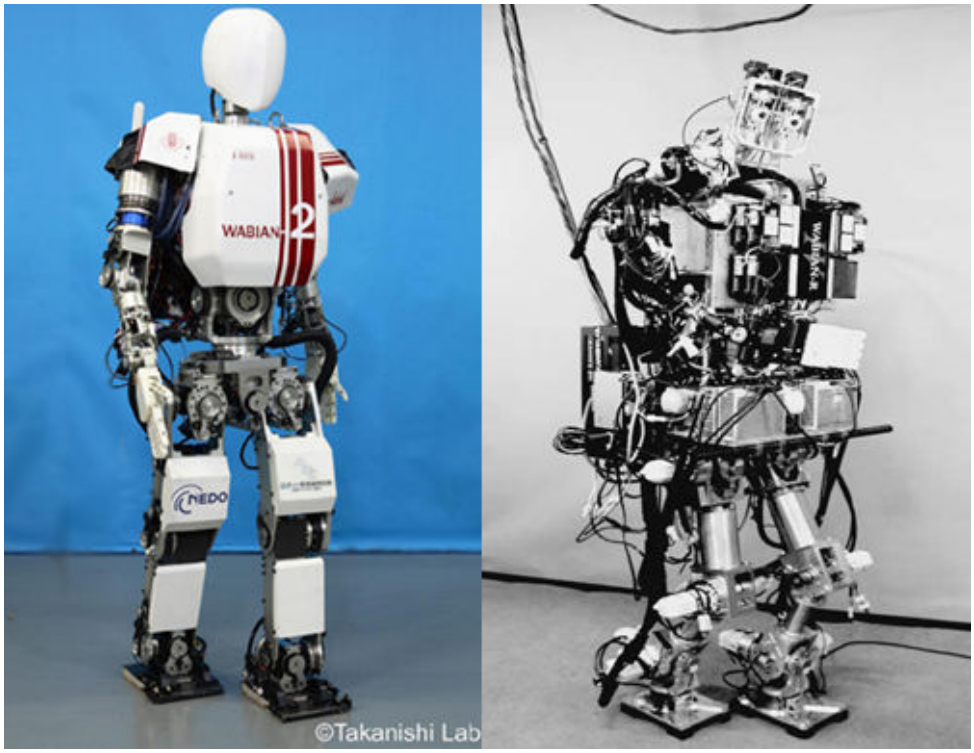

Figure 2.2 WABIAN-RII (left) and WABIAN-RIV (right) Waseda University

In addition to the studies of Waseda University, JSK Laboratory at the University of Tokyo humanoid prototypes H5, H6 and H7 (Figure 2.3). H5 was a child-size full body humanoid robot (30 D.O.F., 1.27 m and 33 kg) built for study of dynamic bipedal locomotion and dynamically balanced trajectory generation [4]. Then, with the motivation of the research on perception-action integration, the humanoid platform H6 (35 D.O.F. 1.36 m and 51 kg) is created with the features like 3D vision and voice

recognition systems. Similar to H6, which is a human-size robot capable of operating autonomously within human environments, the last prototype H7 has 30 D.O.F., 1.468 m height and 57 kg weight [5]. Research on humanoid prototypes H6 and H7 is currently conducted at the JSK Laboratory.

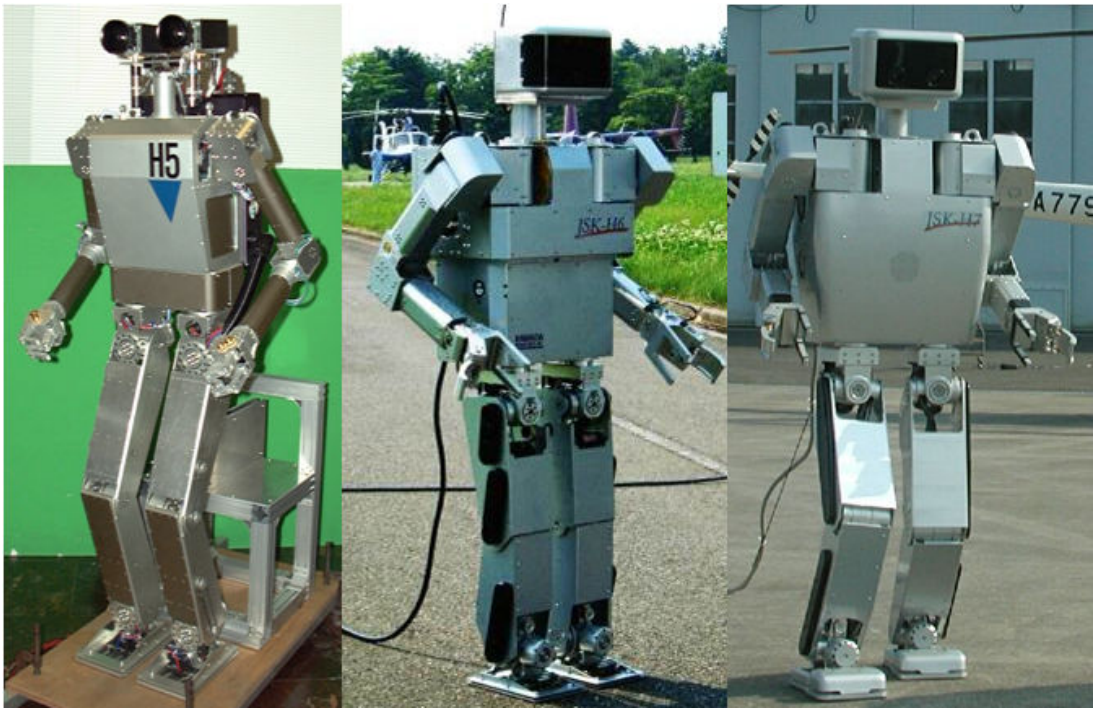

Figure 2.3 H5 (left), H6 (center) and H7 (right) of University of Tokyo

In 2002, Korea Advanced Institute of Science and Technology introduced the new humanoid robot platform KHR-1, which had 21 D.O.F., was 48 kg and 120 cm tall. Stable walking performance is achieved via the use of force/torque and inertial sensors [6]. The 41 D.O.F. second prototype KHR-2, which updated the previous prototypes' mechanical and electrical design followed in 2004. KHR-2 succeeded in vision guided walking and walking on uneven and inclined planes [7]. The final prototype in this context is KHR-3 with the objective of having more human-like features and human-friendly movements, like walking in a self-contained manner powered by embedded batteries, shaking hands and manipulating objects with its five fingered hands [8]. All these three prototypes are shown in Figure 2.4. On the other hand, the same group developed an android type humanoid robot Albert HUBO, which is able to imitate a large variety of facial expressions and HUBO-FX; a human carrying bipedal system.

Figure 2.4 KHR-1, KHR-2 and KHR-3 (HUBO) of KAIST

JOHNNIE, a biped jogging robot by the Technical University of Munich can be mentioned as another successful humanoid research platform [9]. Main objectives of this project are the 3D dynamically stable walking on even/uneven surfaces and fast walking motion up to 2 km/h also called as jogging. The robot has 1.8 m height, 40 kg weight and 17 joints, where the upper body kinematic arrangement consists of only one D.O.F. in the vertical pelvis axis. With the help of its lightweight anthropomorphic structure and feedback from rate gyros and accelerometers at the trunk, stable fast walking and jogging with flight phases up to 2.4 km/h is verified. Then, a performance enhanced version of this prototype; LOLA is developed with an addition of 7 links including elbows, waist and toes to improve walking quality. Current research is conducted on vision guided walking with its multi-focal vision system with four cameras and 6 D.O.F., which will provide a high quality perception and precise navigation in large environments [10].

Since 1986, HONDA has a significant place in the research on humanoid robotics and aroused world's interest by developing the most fascinating humanoid robots (Figure 2.5). With the initial prototypes E0, E1, E2 (by which the first dynamic walking is achieved), E3 the fundamentals of bipedal walking is analyzed and with prototypes E4, E5 and E6 the stability of the walking is increased further by the control techniques developed for posture balance [11]. After the development of the first

human-like model P1, in 1996 the next prototype P2 is introduced to public, which is known as the first self-regulating humanoid walking robot by wireless techniques. P2 was able to walk independently, go up and down stairs and perform various manipulation tasks without wires. With this stunning development, the next prototype P3 was focused on the increase on the robot's reliability and the evolution in size and weight to be more suitable to human environment. The height of the robot is reduced from 1.82 m to 1.6 m and the weight is reduced from 210 kg to 130 kg by this downsizing and the change of the construction material from aluminum to magnesium.

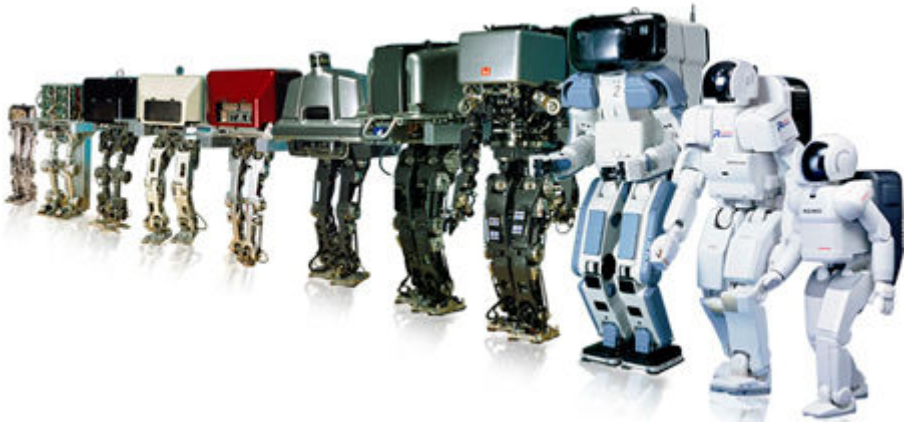

Figure 2.5 HONDA humanoid robots family; (from left to right) E0-6, P1-3, ASIMO

After the experience gained by P2 and P3, the last humanoid robot ASIMO (**A**dvanced **S**tep in **I**nnovative **MO**bility) is introduced in 2000. This robot was more human-friendly than the previous prototypes and have smoother human-like motion capabilities. The sizes of this robot are 1.2 m in height and 43 kg in weight. By the improved walking technology, wider arm operating capabilities and its compact and lightweight structure, it can perform various tasks freely in human living environment. By the new walking technology called i-WALK; a more intelligent, real-time, flexible walking technology leads ASIMO to walk and run continuously while changing directions and interacting with the environment [12]. On ASIMO, research on many topics, including human-robot interaction and new artificial intelligence systems about learning and decision making are conducted by humanoid robotics researchers around the world.

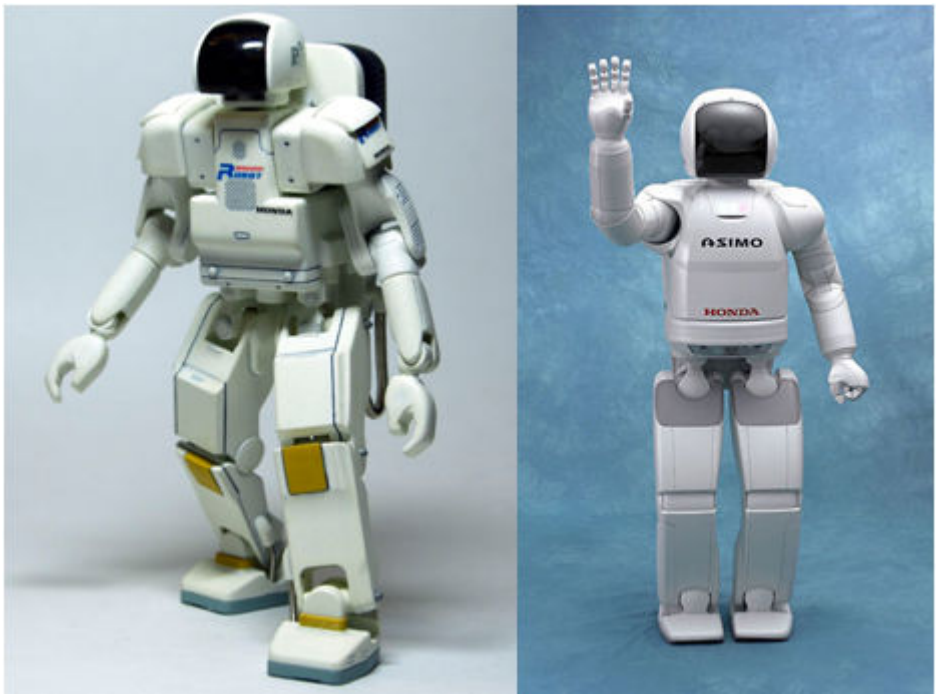

Figure 2.6 P3 and ASIMO of HONDA

In 1998, The Ministry of Economy and Industry (METI) of Japan started the Humanoid Robot Project (HRP) with the aim of developing humanoid robots that perform manual labor in the society. The first prototype HRP-1 was developed by Honda R&D as an enhanced version of prototype Honda P-3, including the controller system [13]. The prototype is 1.6 m in height and 120 kg in weight consisting 30 D.O.F. In 2001, National Institute of Advanced Industrial Science and Technology (AIST) developed their own control system, which enables the control of both arms and legs simultaneously and called this prototype HRP-1S. This prototype is employed in the teleoperation of industrial vehicles and care of patients. The second platform of the project, HRP-2 started with the leg module HRP-2L, the arm module HRP-2A and a prototype HRP-2P. Improving these modules resulted in the introduction of HRP-2, having a more lightweight (1.54 m and 58 kg) and compact body with no backpack. This robot is widely used as a research and development tool for humanoid robotics. The last platform developed by AIST is HRP-3, which firstly presented with the prototype HRP-3P. The mechanical and electrical system of this platform is designed to perform in rough and dangerous working conditions like rain and dust. HRP-3 is presented with the addition of newly designed hands and wrists to improve manipulation capabilities [14]. The planned application areas of these robots can be

listed as; maintenance tasks of industrial plants, guarding of the home and offices, teleoperations of construction machines, care of patients in beds and cooperative works with human or robot in working environments [13].

Figure 2.7 HRP 2 (left) and HRP-3P (right)

Another example of humanoid robotics can be given as CB-i, DB2 and i-1 platforms developed by SARCOS Company. This project is conducted by JST (Japan Science and Technology Agency) ICORP, Computational Brain Project and ATR Computation Neuroscience Laboratories with the motivation of research on computational brain functions and to realize skillful human behaviors on humanoid robots. The CB prototype has 50 D.O.F, 1.575 m height and 92 kg weight [15] and is actuated by hydralic actuators (Figure 2.8). The studies of this humanoid robot is mostly based on understanding of the biological principles of human bipedal locomotion and designing control alrogithms on the computational principles of the human brain. Realization of human-like walking performance, 3D balancing, physical interactions visual processing based perception are the main subjects of this project. Gravity compensation, which makes the robot passive to any external forces and full-body balancing of the humanoid robot with passivity based force control have been achieved.

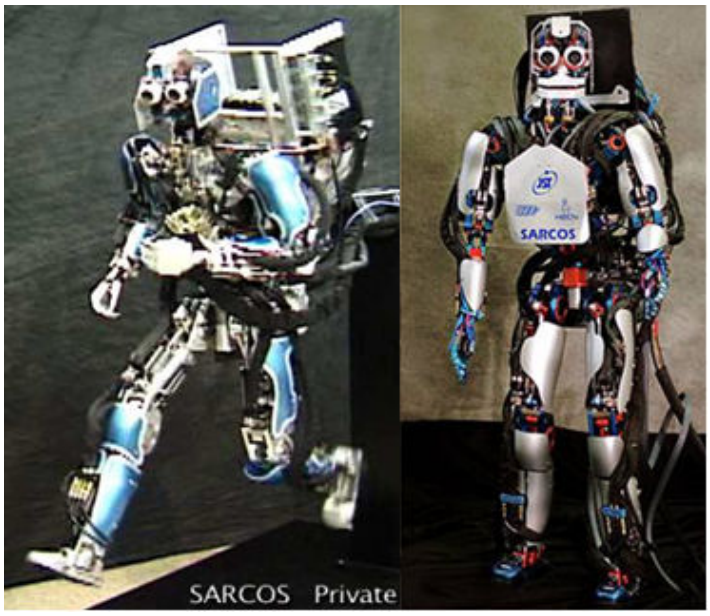

Figure 2.8 DA ATR DB2 and CB-i humanoid robots of SARCOS

In addition to the human-size humanoid robots, small size platforms are developed too. In 2000, Sony developed a child-size humanoid robot SDR-3X (Sony Dream Robot-3X) which has 24 D.O.F., 0.5 m height and 5 kg weight [16]. Although this platform is developed for entertainment purposes, in addition to its stable walking, with the help of its developed balance control algorithm, it can perform highly skilled whole body motions, such as sitting down on the floor, standing up from a bench, kicking a ball, standing on one leg, dancing in various tempos and other perception features like voice recognition and color detection. This robot is further developed to platforms SDR-4X; providing more features like terrain-adaptive motion control, real-world space perception and multi-modal human-robot interaction [17] and QRIO (SDR-4XII), which is known as the first running biped robot at 23 cm/s in 2005.

Many other examples can be given for small-size humanoids. The child-size robot HOAP-2 engineered by Fujitsu Automation Ltd, Japan was 50 cm tall and weighing 7 kg, and introduced by the objectives; developing motion control algorithms for bipedal walking and human-robot communication interfaces [18]. Besides the use as an efficient development tool, it was also imitating whole-body human motions like standing up and performing martial arts.

PINO developed by Japan Science and Technology Corporation, Inaba's remote brained humanoid robots, SAMSUNG's MAHRU-3, Kondo Kogaku's KHR, General Robotix' HRP-2m, VSTON's VisiON4G are among known examples of small-size humanoid robots [19].

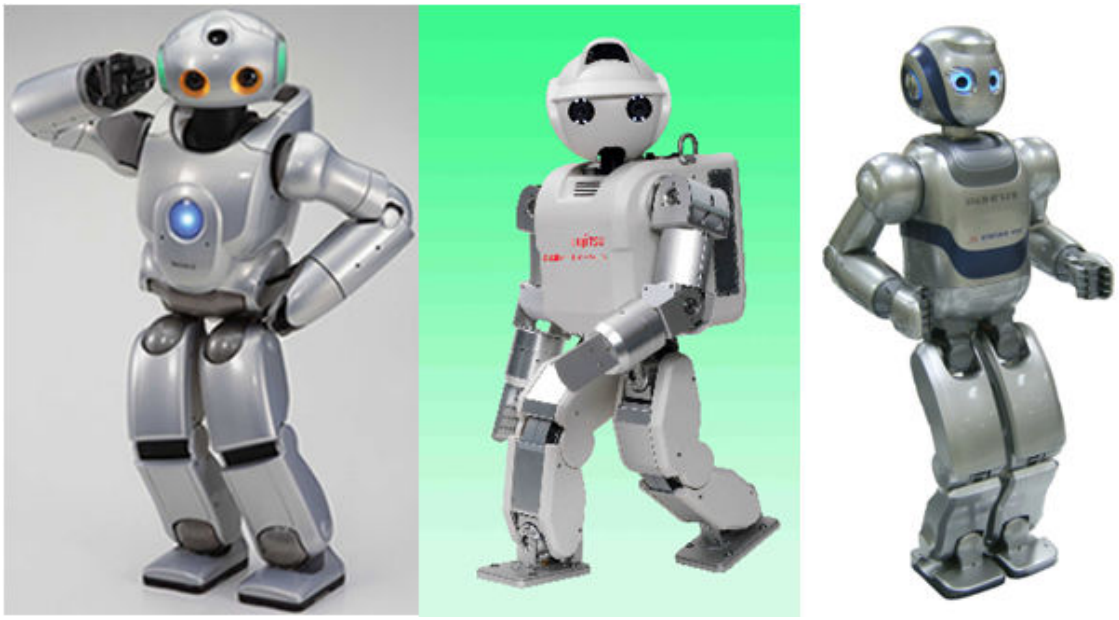

Figure 2.9 Sony QRIO (left), Fujitsu HOAP-3 (center), MAHRU-3 Samsung (right)

2.2. Humanoid Locomotion Terminology

Over the past several decades, the human locomotion attracts many humanoid robotics researchers all around the world. This study on the bipedal locomotion requires the understanding of the basic fundamentals of the gait. The locomotion can be investigated in three reference planes in order to simplify the analysis of the human motions. These reference planes can be shown as in Figure 2.10 [20]. The analysis of the human walk is mostly based on the sagittal and the coronal planes. The sagittal plane is on the direction of the walk. The coronal plane, also called frontal plane is considered in the lateral walk studies. The balance of the robot body is investigated in both coronal and sagittal planes.

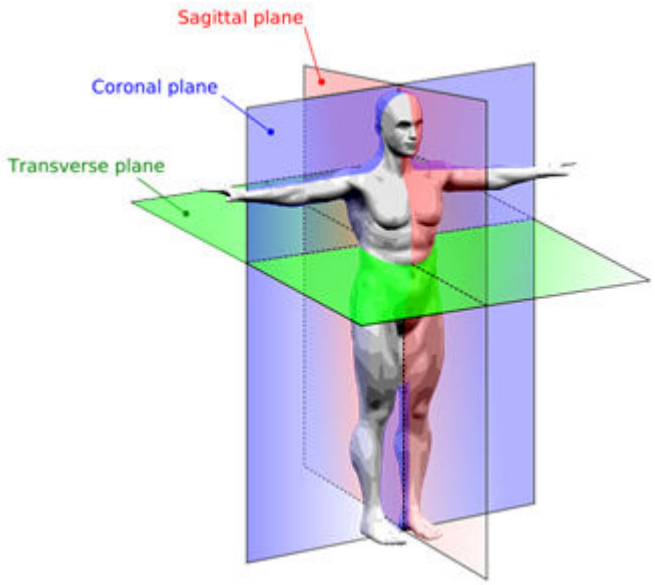

Figure 2.10 Body reference planes

A walking cycle can be divided into phases [21]. One gait cycle is composed of two double support and two single support phases (Figure 2.11). In the double support phase, both feet are in contact with the ground and in the single support phase, only one of the feet is on the ground. In the single support phase, the foot on the ground is in the support phase, while the other one is in the swing phase. The sum of the single support phase and two double support phases of one foot which is on the ground is the stance phase. Moreover, the swing foot has a take-off and a landing phase in the swing phase. These phases have a crucial role in trajectory generation and balance control algorithms.

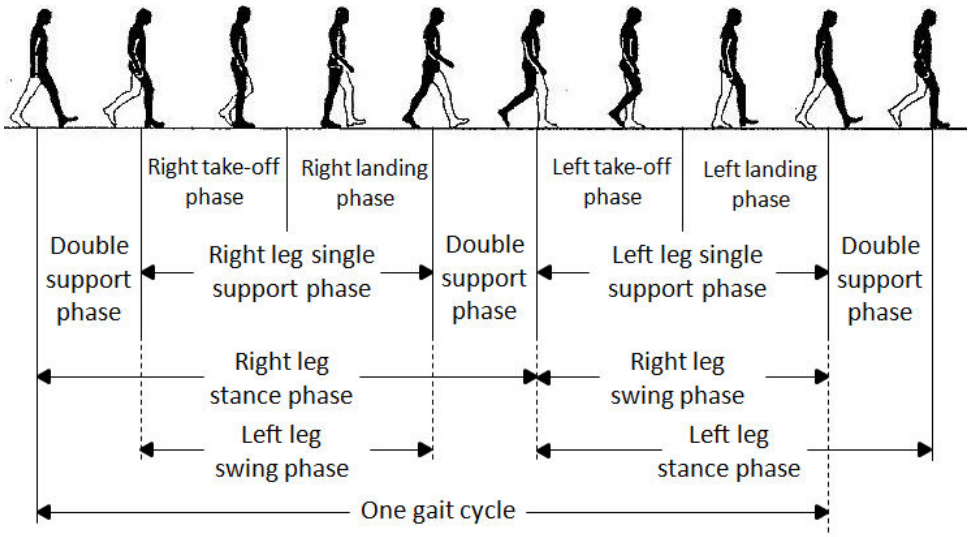

Figure 2.11 Walking phases

Step size and stride length are important parameters in the trajectory generation. The step size is the additional distance covered by the swing foot with respect to the support foot, and the stride length is the total distance covered by the swing foot. Swing offset is the distance between the ankle centers of the feet (Figure 2.12).

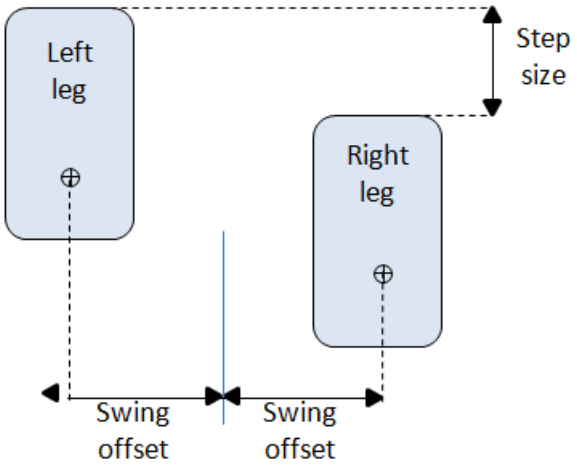

Figure 2.12 Step size and swing offset

In 1968, Vukobratovic introduced the ZMP (Zero Moment Point) Criterion and this concept is widely used on the stability analysis of the humanoid robot walk. ZMP is defined as the point P on the ground where the sum of all moments of active forces with respect to this point is zero [21]. This definition is based on the idea that the pressure under the supporting foot can be represented by the appropriate force acting at a certain point. The location of the Zero Moment Point is used as an indicator of stability in bipedal walk.

2.3. Literature Review on Humanoid Walking Trajectory Generation

Bipedal locomotion is a challenging task due to the many degrees of freedom, coupling effects between them and the robot's highly nonlinear dynamics. Vukobratovic et al. proposed numerical calculation methods for generating walking trajectories for biped dynamic walking [21], which was studied by Takanishi et al. in order to realize a dynamic walking using a similar approach [2]. Altough the robot WL-10RD was successful in dynamically stable walking however the computational effort and time was enormous and the adaptation to the environment was very poor in real time. There was the need for efficient ways of obtaining reference trajectories by simplifying these models. Successful results have been obtained by many humanoid robotics researchers during the last four decades, however these studies still lack in reliability, safety in human environment, motion capability and full-body stability compared to human.

The ZMP concept is one of the most famous techniques in trajectory generation of humanoid robotics. First humanoid robots in ZMP scheme used multiple rigid body models [2]. Kaneko et al. propose an offline walking pattern generation method based on the ZMP criterion assuming that the robot and environment model is known [22]. This walking pattern includes the off-line generation of the foot and the hip trajectories. The foot trajectories are computed by a 3^{rd} order spline interpolation, considering the kinematic constraints and that the derivatives of the position and angles are continuous at all these constraints to derive smooth curves. Same idea is applied to hip trajectories to have a smooth body motion with large stability margin.

Since the whole characteristics of the robot is considered in these approaches, although the trajectories were precise, the computational cost was high and hard to adapt online. Therefore, another approach in ZMP scheme has been proposed by Kajita et al. [23]. This approach uses on a 3D Linear Inverted Pendulum Model assuming that the whole robot mass is concentrated as a single mass at the robots center of gravity (COG). This simplified model does not require the whole model of the robot and thus is computationally effective. In order to keep the simplicity and linearity in the dynamic equations of the robot, the height of the center of mass position is kept fixed. By this

assumption, the equations of motion for the LIPM are decoupled into sagittal and coronal planes, where the dynamic equations for each plane can be written by using a 2-D Linear Inverted Pendulum Model for x-z and y-z planes.

These approaches verified the effects of the Zero Moment Point on the dynamic stability of the humanoid robots and this criterion has been used by many researchers around the world. The ZMP criterion is used in the trajectory generation of other humanoid robot platforms too [1, 5, 17, 24].

Many other ideas exist on trajectory generation. One of them is the biologically inspired technique called Central Pattern Generator [25]. In this approach, it is assumed that the locomotion is composed of synchronized rhythms of different gaits and the idea is that these synchronized periodic motions can be generated using self oscillatory systems, which do not require inputs. The studies on this approach may be divided into two categories [26]. The first group proposes that the walking is generated by the synchronization of signals assigned to each joint. In order to synchronize these joints, the walking is separated into phases and the joints are mapped to the movement features of each leg, such as leg extension, leg angle and foot angle. The other group proposes the generation of each signal centered by neural network systems. This neural oscillator system may be composed of a Central Pattern Generator to generate voluntary and involuntary motion patterns, an adaptive neural network to modify motion patterns depending on ground conditions, a knowledge base to store walking parameters and a switch mechanism to make decisions between voluntary and involuntary motions [27]. Studies can be listed on the application of this approach on bipedal locomotion [28-30].

The trajectories for bipedal walking might also be computed as parametric functions. This will require that the references of the selected points on the robot (e.g. foot, hip, torso and so on) are parameterized and will be calculated for every phase of the gait. In these approaches, the mathematical functions can be time dependent, which will generate periodic and synchronous motions for the limbs. The computation of these functions also requires the consideration on various kinematic or dynamic constraints. Using this approach will simplify the computation of the trajectories and provide flexibility in the online adjustment of these parameterized trajectories. Similar techniques on trajectory generation are employed in the following humanoid robot platforms.

Oh et al. proposed a walking pattern generation method based on the computation of Cartesian coordinate references of the pelvis and two feet, on the

humanoid robot KHR-2 [31]. Their walking pattern design is generally based on the walking period, the ratio of double/single support phase, step size and lateral swing amplitude of the pelvis. By the determination of these parameters, the trajectories for the feet are generated with respect to a body fixed coordinate system attached to the pelvis. Moreover, the trajectories for the pelvis are generated by computing the absolute position of the pelvis with respect to a ground-fixed coordinate system. The lateral trajectory of the pelvis and the *z*-direction trajectories of two feet are generated by cosine functions to produce a smooth curve. The forward (*x*-direction) trajectories of two feet with respect to the body fixed coordinate system are generated by a cycloid function as a combination of cosine and linear functions. Improvements on this walking pattern generation are presented in [8] on the humanoid platform KHR-3. In this technique, it is planned that the walking parameters are minimized for easy operation and better tuning performance, the trajectory curves are smooth and continuous due to their simple analytic form and easy to implement in real time by less computational burden. The trajectory synthesis is composed of two main categories; a cycloid function for the computation of ankle positions in Cartesian space and a 3^{rd} order polynomial function for pelvis position. The main contribution of this study is the online adaptation of the walking pattern depending on the position and velocity boundary conditions determined as inputs from the operator or from the navigation algorithm.

Kawamura et al. from Yokohama National University proposed a similar trajectory generation algorithm, which is based on the computation of foot positions and orientations with respect to a coordinate frame located on the torso [32]. The Cartesian foot references are computed by simple sinusoidal functions in the *x, y* and *z* directions. In 2004, this trajectory generation method is improved with the general rule that the feet land the floor with zero velocity with respect to the floor [33]. The forward/backward and lateral motion (*x* and *y*-direction) of the feet with respect to the torso is computed with a 5^{th} order polynomial with six constraint conditions of position, velocity and acceleration in start and finish times of the walk. In *z*-direction, trajectories are computed by a 6^{th} order polynomial function considering seven constraints; the height of the foot, the lift-off and landing velocity, lift-off and landing acceleration are zero at the beginning and end of swing phase and swing foot reaches its peak at the half of the swing phase. This trajectory also assumes that the orientations of the feet are parallel to the ground and guarantees that the robot torso moves with no acceleration.

A trajectory generation method similar to [32] is presented by Erbatur and El-Kahlout [34] who propose a walking pattern adaptation technique to compensate the sudden addition of loads of unknown masses and Erbatur and Bebek [35] who propose an online fuzzy adaptation scheme for a walking parameter in the offline generated walking pattern.

Similar to [34] and [35], this thesis presents a reference generation method based on parametric functions. The major contribution of this thesis in the context of reference generation is the smoothening of the foot trajectories and the introduction of the ground push motion of the feet in the vertical direction, which dramatically improved the stability of the robot in the take-off phase.

2.4. Literature Review on Humanoid Walking Control Algorithms

One of the most challenging problems in this field is the robust balance of the walk due to the nonlinear and hard-to-stabilize dynamics of the free-fall robot and the coupling effects between the many degrees of freedom. These complications require online control algorithms in order to maintain the dynamic stability of the robot during the walk. It becomes even more important to conserve the balance of the robot posture in the case of walking on an uneven and inclined terrain. In the humanoid robots literature, the researchers have developed various walking control algorithms using the sensory feedback from force/torque sensors, inertial sensors, such as accelerometers, gyrometers and inclinometers, and visual sensors.

A simple categorization can be given for these types of sensors in three levels [6]. The first level is the F/T sensors at the wrist and ankle joints and these sensors are enough to ensure the stability of the walk on a flat surface. The second level is the accelerometers, rate gyros and inclinometers, which gives the sensory data about the equilibrium of the upper body. This second level is required to maintain the balance of the robot posture and to improve the quality of the walk in the existence of environmental disturbances and unevenness of the ground. The third level sensors are the vision sensors, providing the space perception and making the interaction with humans possible.

Walking control algorithms can be divided into two main categories. In the first one, the walking trajectory references are modified based on the sensory feedback. In this category, the control technique acts to the walking trajectory generation and the joint references are computed depending on the new modified reference trajectories. On the other hand, the control algorithms in the second category apply directly to the joint references computed from the walking trajectory generation. These types of control techniques can be shortly stated as the compensation onto the joint reference trajectories based on the sensory information.

The first examples of the control algorithms can be given as the work by Takanishi et al. [2, 36, 37]. This study in Waseda University is based on a control method on dynamic bipedal walking based on the compensation of Zero Moment Point trajectories in roll, pitch and yaw axes by trunk and waist motions in these three axes. In

1985, with the biped robot prototype WL-10RD (Waseda Leg-10 Refined Dynamic), dynamic walking on uneven surface is succeeded with an inclination of 5 degrees on the surface. However, this prototype consisted of only the lower limbs and in order to increase the limited walking terrain adaptability and to satisfy the dynamic stability of the robot walking, in 1986, WL-12 (Waseda Leg 12) is developed which has a trunk for the stabilization of the walk. The control algorithm in [36] and [37] is based on the compensatory motion control using waist and trunk joints, which cancels the moments (in roll, pitch and yaw axes) generated by the robot motion. By using these techniques WL-12III and WL-12V realized faster and more stable walking on flat and uneven surfaces [36, 37].

Hirai et al. from Honda humanoid research group introduced walking balance control techniques developed to maintain the stability of the robot posture and tested on the humanoid robot prototype P2 [24, 38]. Two main control methods applied before the walking pattern generator are called “Model ZMP Control” and “Foot Landing Position Control”. The Model ZMP Control has the aim of modifying the desired ZMP to an appropriate position in order to keep the robot posture stable. Depending on the inclination of the upper body, the ideal body trajectory is changed when the robot is about to lose balance. This control works by increasing the desired inertial force by accelerating the upper body position forward and backward. Foot Landing Position Control changes the position of the landing foot depending on the changes due to the Model ZMP Control. After the recovery of the robot posture by the Model ZMP Control, the distance between the upper body and the landing foot position changes and Foot Landing Position Control modifies the step size. Another example to the control algorithms, which apply directly to the joint references after the walking trajectory generation, can be given as a control technique called “Ground Reaction Force Control” which is based on the information from a 6-axis force/torque sensor [24]. This method is based on the compensation of the desired position and the posture of the feet based on the changing ground reaction forces. Depending on the case that the robot body tips forward or backward, this control method recovers the posture by rotating the supporting foot around the desired ZMP. The overall control structure of Honda

humanoid robots can be shown as in Figure 2.13. In [38], these algorithms have been combined under the title "Macro Stabilization Control" and explained in more detail.

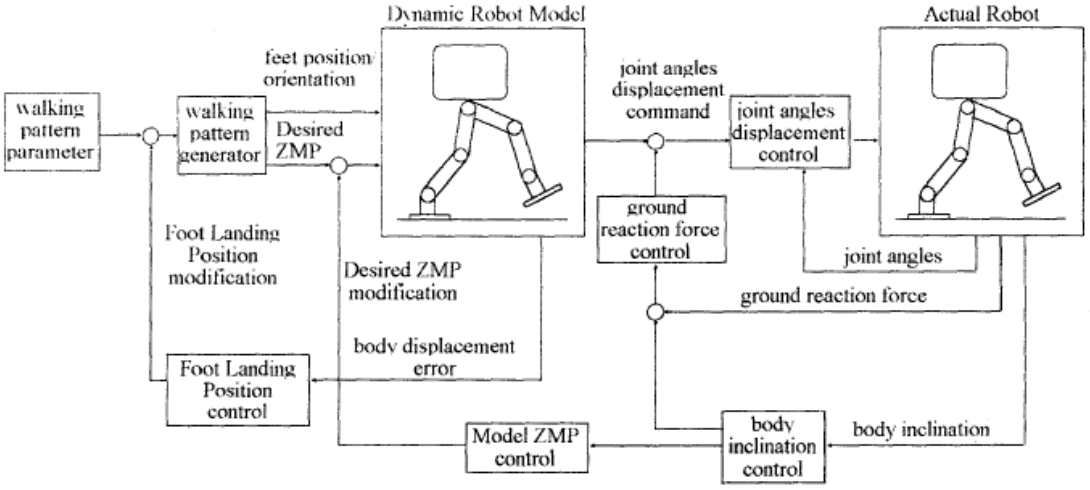

Figure 2.13 Overall block diagram of walking control algorithms of Honda humanoid robot [24]

Examples on the control algorithms may be extended to the work of KAIST Research group, which developed online balance controllers to realize stable walk on humanoid robots KHR-1 and KHR-2. A similar method to "Foot Landing Position Control" introduced by Honda research group is proposed by KAIST Humanoid Research Group with the name "Landing Position Controller" [6]. This method is based on the idea that the actual landing time and position of the swing foot may be different from the prescribed values due to the unevenness of the terrain. If the landing occurs before the desired time, the position references of the landing foot is modified and the unexpected movements in the x and z axis are prevented. Another technique called the damping controller is developed to compensate the position error because of the oscillation to an impact force on the foot. It is claimed that this oscillation is mainly due to the compliance at the humanoid leg, which is controlled considering the stiffness of the links by modeling the system as a single mass inverted pendulum with a compliant joint as shown in Figure 2.14. In this figure, u represents the ankle joint reference angle, θ denotes the actual ankle angle due to the compliance and T is the torque at the ankle

read from the F/T sensor. A feedback controller to compensate this compliance has been developed and the ankle joint references are modified.

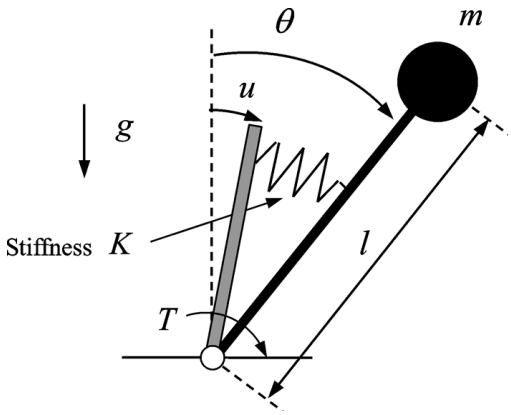

Figure 2.14 Simple inverted pendulum with a compliant joint [6]

The third controller proposed by Jun Ho Oh et al. is the landing orientation controller, which is based on the difference between the actual and the prescribed angle of the swing foot. In order to prevent the instability due to the imperfect contact of the swing foot and reduce the impact due to landing, the reference ankle position is controlled such that the swing foot has a stable ground contact. In 2007, Jun Ho Oh et al. [7] proposed a more developed walking control algorithm for walking on uneven and inclined floor instead of the assumption that the walking surface is perfectly flat. One of the two main controllers proposed is the upright pose controller to prevent the tilting of the robot towards the inclined walking surface and to keep the upper body of the robot straight independent of the ground conditions by measuring the floor inclination from the inertial sensors mounted on the robot torso. In addition to this method, a shock absorber algorithm is introduced with the aim of compensating the local unevenness of the walking floor. This algorithm is based on the idea that if the swing foot lands before the desired time due to the changing ground conditions, the height of the hip joint is modified to absorb the landing impact, depending on the measured ground reaction force. Adding these algorithms onto the ones in [6], the humanoid platform KHR-2 shows successful walking results on various uneven terrains.

In 2000, Kaneko et al. proposes that even though a highly stable, smooth walking pattern is generated offline, in order to adapt irregular rough terrains or unexpected external forces, a real time modification is required [22]. It is claimed that in the motion trajectory generation it is quite difficult to model all the nonlinearity, compliance effects and the working environment. In order to compensate these factors, the proposed stabilizing control consists of three main elements. Firstly, a body inclination control is proposed, which is based on the adjustments on the hip angle to overcome the difference between actual and desired body posture angles, obtained from accelerometer and rate gyros. Secondly, to avoid improper contact of the foot, the actual ZMP must be kept in the stability region (Figure 2.15), as mentioned in Section 2.2. Relying on the information from the force/torque sensors at the feet, the most effective way is asserted to be the control of the ankle joints of the support foot. Furthermore, the landing of the foot may be too late or fast than the planned walking pattern and this would cause the robot to tip forward and backward, due to the moment created during the contact. If the landing times are different in the actual and ideal walking, this is controlled by lowering or heightening the landing foot with a proportion to the reaction force.

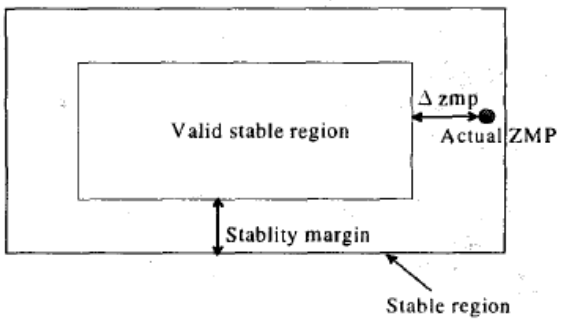

Figure 2.15 Stable regions of ZMP [22]

In 2001, the research group further developed their control strategies in collaboration of AIST and Honda R&D Co. Ltd. On a humanoid robot platform produced by Honda, they developed their own software structures and implemented their control algorithm. In [39], same problems on the stability of walk are emphasized and developments on the techniques in [22] are presented. It is proposed that body inclination may be controlled by adjusting the position and orientation of the feet instead of the hip joints and here the body angles are estimated by a Kalman filter using the information from gyroscopes and G-force sensors. Moreover, In the ZMP control,

the error between ideal and actual ZMP is compensated by accelerating the torso of the robot. Also, for inclined and rough terrains a foot adjusting control technique is introduced. With the controllers proposed above, the stable motion of HRP1S is achieved. Further developments on the control structure of the same humanoid robot "HRP" are presented by Yokoi et al. which include a whole body posture controller based on inertial forces to increase the full-body motion capabilities of the humanoid robot [40].

Kagami et al., researchers from the University of Tokyo, introduced a strong and inspiring online balancing algorithm for maintaining dynamic stability of the humanoid robot, called "Autobalancer" [41]. The developed software generates a modified dynamically stable motion for a given input trajectory and environment conditions. Two parts of this algorithm are a planner for state transitions based on robot-ground contacts and a full-body dynamic balance compensator which compensates the deviations from the centroid position and moments generated by any motion of the robot. This generic algorithm solves the balance problem as a constrained 2^{nd} order nonlinear optimization problem and has the flexibility of developing the algorithms for varying D.O.F.s and constraint equations [41]. The experiments are conveyed with the robot platform H5. In 2006, Inoue et al. from the same research group presented the layered control system used in the experiments of H7 [5]. This system provides a structure for high-level autonomous locomotion behaviors, including a low-level trajectory modification to compensate modeling errors and sudden changes in the walking environment. Control methods discussed in [5] start with the modification of the torso position to compensate the errors in the ZMP, similar to the technique explained in [39]. The deviation of the hip joints in the roll axis is corrected using the information from rate gyros. Finally, the impact generated at the foot landing is absorbed by adjusting joint servo gains, using the contact timing information. By the help of these algorithms, the balance of the robot is maintained in locomotion and other complex autonomous behaviors.

Apart from the walking control algorithms explained above, other methods are published too. One of the major techniques is compensation of the angular momentum of the robot, which is created by the inertial effects or the reaction forces exerted on the robot [42-45]. In these works, angular momentum based inverted pendulum models or direct feedback of angular momentum are employed to manipulate the CoM trajectories.

Chapter 3

3. THE HUMANOID ROBOT: SURALP

3.1. Mechanical Design of SURALP

The humanoid robot: SURALP used in this thesis is designed and constructed in the framework of a TUBİTAK funded project (106E040). The 29 D.O.F. full-body robot with the control hardware integrated in its trunk is shown in Figures 3.1 and 3.2. The robot is designed to be realistic in human proportions and adaptable to human environment.

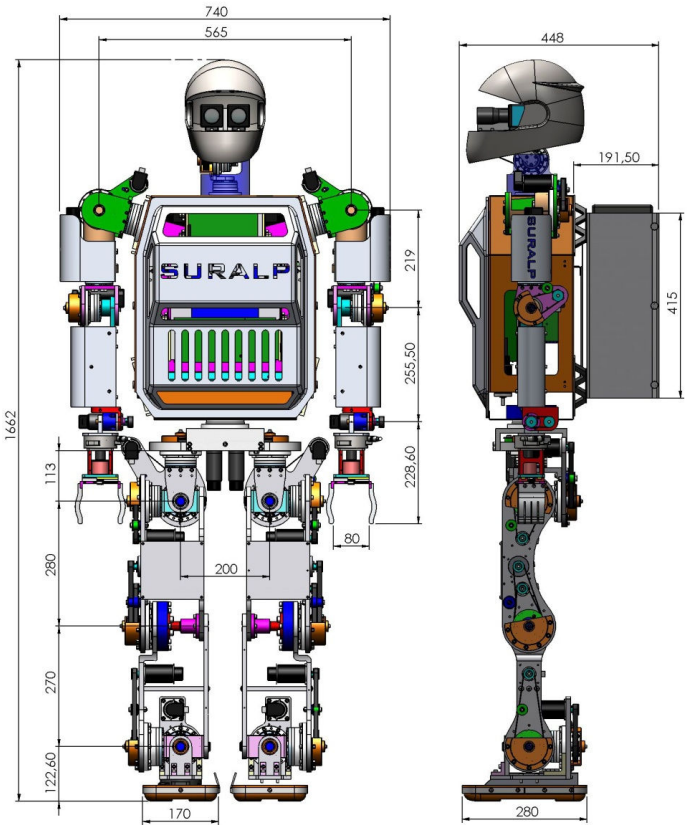

Figure 3.1 Dimensions of SURALP [mm]

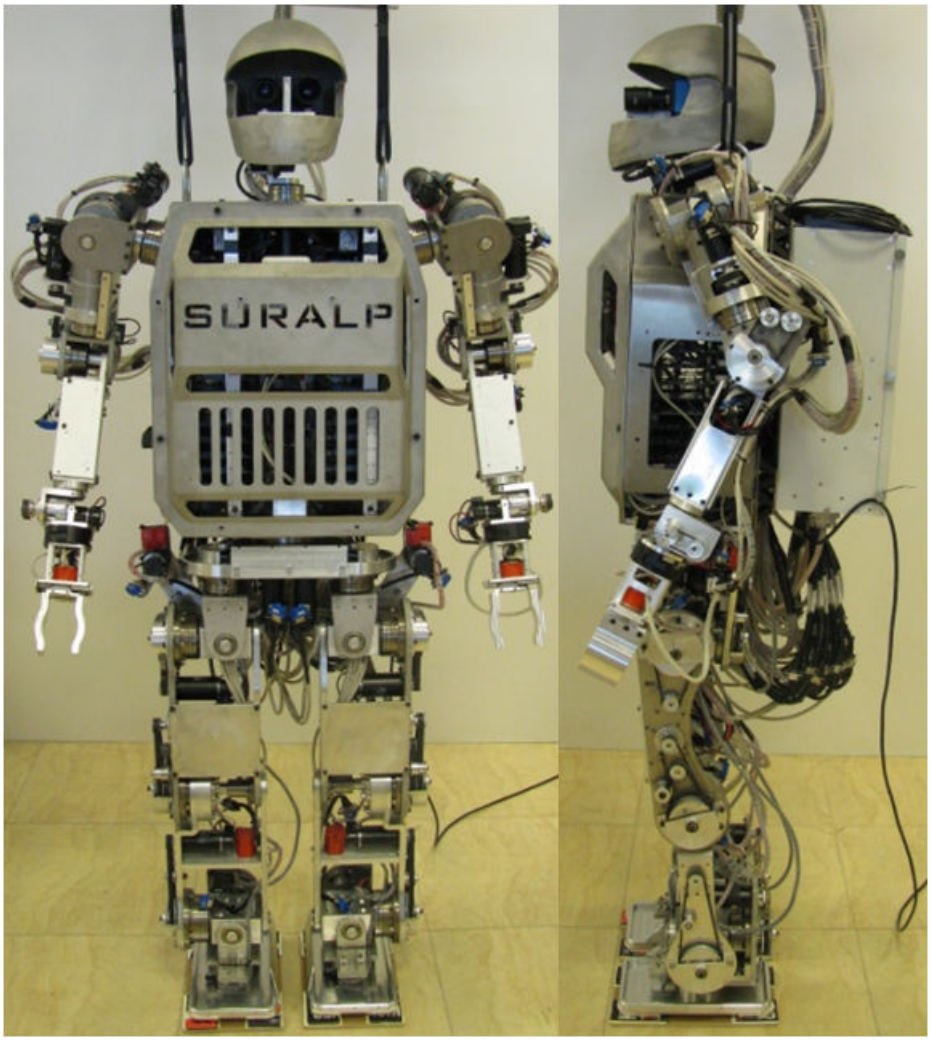

Figure 3.2 Front and side views of SURALP

The hip is composed of three orthogonal joint axes which intersect each other at a common point; hip center. In the kinematic arrangement, the knee axis follows the hip pitch axis. The ankle accommodates ankle pitch and ankle roll axes, which are orthogonal [46]. A waist yaw axis is positioned on the pelvis. The arms are designed as 6 D.O.F manipulators with the following axis arrangement. The shoulder motion is realized by three orthogonal joint axes followed by a revolute elbow joint. In order to actuate the wrist, a roll and a pitch axis is positioned in the forearm of the robot. The single D.O.F hand opens and closes with a linear motion. The neck is composed of two joints in the pan-tilt configuration. The whole kinematic arrangement of the humanoid robot is shown in Figure 3.3.

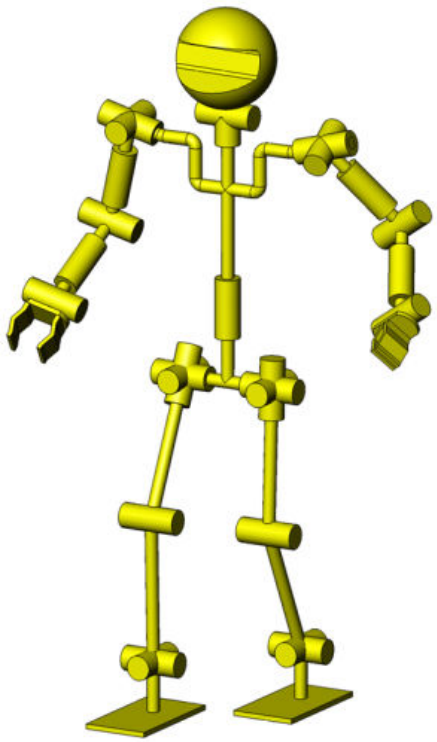

Figure 3.3 The kinematic arrangement of SURALP

The link length and weight information is tabulated in Table 3.1. 7000 Series aluminum is chosen as the construction material. Except the knee joint, all joints have a single DC motor actuation mechanism. The knee joint is driven by two DC motors for high torque capability. Belt-pulley systems transmit the motor rotary motion to Harmonic Drive reduction gears. The joint motor power capabilities, reduction ratios of belt-pulley systems and the Harmonic Drives are displayed in Table 3.2. In addition, the working ranges of the joints are added to this table.

Table 3.1

Length and weight parameters

Upper Leg Length	280mm
Lower Leg Length	270mm
Sole-Ankle Distance	124mm
Foot Dimensions	240mm x 150mm
Upper Arm Length	219mm
Lower Arm Length	255mm
Robot Weight	101 kg

Table 3.2

Joint actuation system

Joint	Motor Power	Pulley Ratio	HD Ratio	Motor Range
Hip-Yaw	90W	3	120	-50 to 90 deg
Hip-Roll	150W	3	160	-31 to 23 deg
Hip-Pitch	150W	3	120	-128 to 43 deg
Knee 1-2	150W	3	160	-97 to 135 deg
Ankle-Pitch	150W	3	100	-115 to 23 deg
Ankle Roll	150W	3	120	-19 to 31 deg
Shoulder Roll 1	150W	2	160	-180 to 180 deg
Shoulder Pitch	150W	2	160	-23 to 135 deg
Shoulder Roll 2	90W	2	120	-180 to 180 deg
Elbow	150W	2	120	-49 to 110 deg
Wrist Roll	70W	1	74	-180 to 180 deg
Wrist Pitch	90W	1	100	-16 to 90 deg
Gripper	4W	1	689	0 to 80 mm
Neck Pan	90W	1	100	-180 to 180 deg
Neck Tilt	70W	2	100	-24 to 30 deg
Waist	150W	2	160	-40 to 40 deg

With the aim of absorbing some of the impact during the interaction of the feet with the surface, a mechanical solution is proposed. Various foot designs with soft rubber materials at the bottom are tested and the walking performances with these feet have been compared. Despite soft materials absorb an important amount of the impact generated at the sole of the foot, very soft designs caused the robot foot to slip on the ground and resulted in a serious loss of stability. In the final design of the sole, a more human-like foot is aimed and the best walking performances are obtained with this design (Figure 3.4)

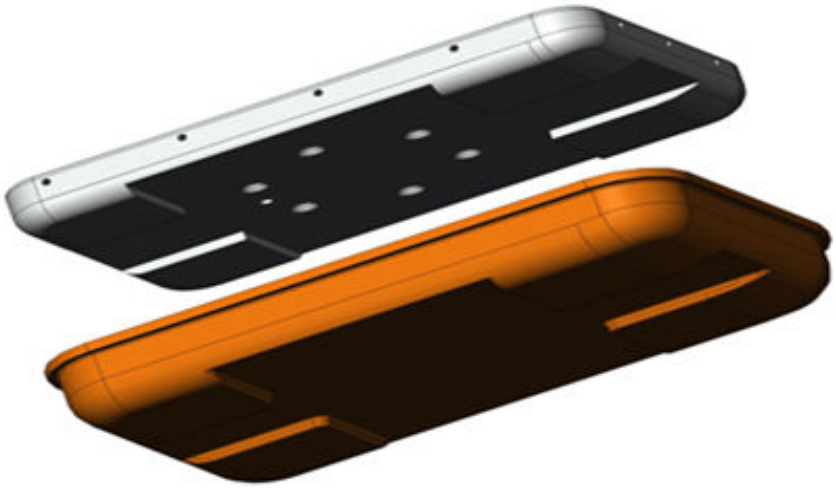

Figure 3.4 The bottom view of the final sole design

3.2. Sensory System

The sensory system of SURALP is composed of sensors in the following four categories:

i) Joint encoders

ii) Force and torque sensors

iii) Inertial sensors

iv) CCD cameras

The motor angular positions are measured by 500 pulses per revolution optic incremental encoders mounted to the DC motors.

Two kinds of force and torque sensors have been used throughout the project. One is the 6 axis force/torque sensor which is positioned at the ankle of the robot. An alternative force and torque measurement system is obtained by the use of FSRs (Force Sensing Resistors).

FSRs are polymer thick film devices showing a decrease in their terminal resistance by increasing the force applied to their active surface. The dimensions of the sensors used are 40 mm x 40 mm x 0.43 mm and their weight is negligible. The very thin structure enables assembling without an increase in the foot height and a wide range of forces can be measured with a large contact area. The resistance values of the sensor for varying force values from 0-25 kg are plotted. It is observed that the resultant curve is highly nonlinear and a piecewise linear approximation is used to obtain force values from the voltage measured at the terminals of the FSRs. Figure 3.5 illustrates the placement of the four FSR sensors under the robot foot. The layers at the foot sole composed of various materials together with the FSRs are shown in Figure 3.6.

The use of force measurement units at the four foot corners enables us to obtain tactile information about at which corner the robot tilts. The ground interaction force in the vertical direction and the torque values at the ankles can also be measured by this system. The 6 axis force/torque sensors and the FSR based foot corner force sensors are used interchangeably. A difference in the quality of measured signals in terms of drift, response time and accuracy in favor of the 6 axis force/torque sensors is observed. The

control algorithms developed in this thesis are tested and implemented with 6 axis F/T sensors. Still, the FSR sensors are an alternative for walking on uneven surfaces.

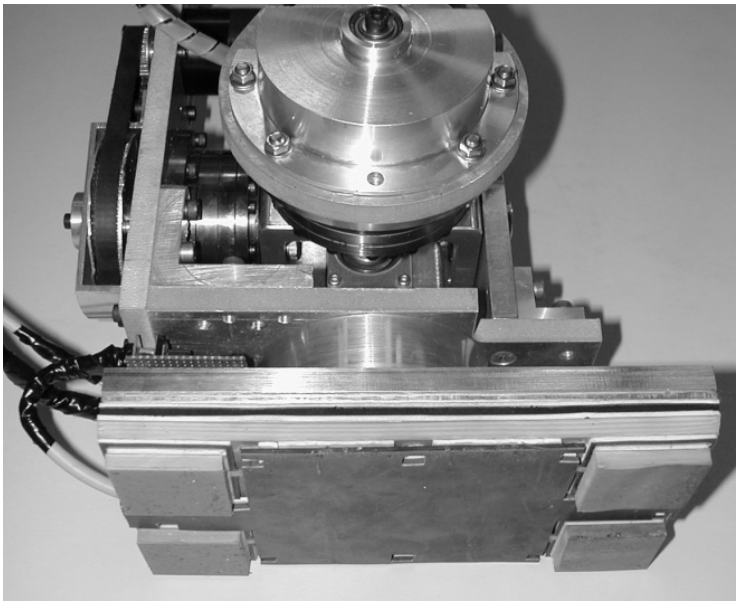

Figure 3.5 The bottom view of the FSR based robot foot sensor

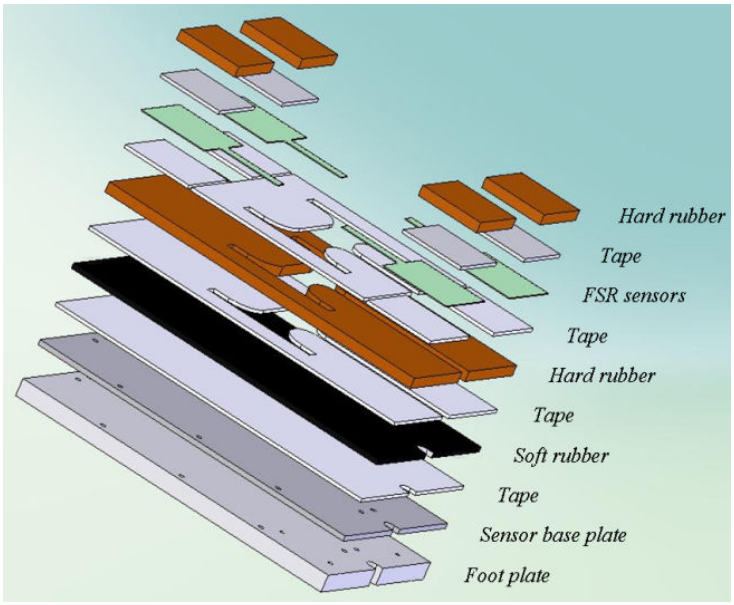

Figure 3.6 Layers of the foot sensor with FSRs.

Three types of inertial sensors are used and compared in this project. A rate gyro, a linear accelerometer and an inclinometer are mounted at the robot torso to obtain roll/pitch angles and angular rates in the roll/pitch/yaw axes. Throughout the thesis, the inclinometer is used for development of control algorithms related to the body inclinations and its performance was satisfactory.

Two Firewire CCD cameras are mounted to the robot head for visual information.

These sensors are listed in Table 3.3 with their working ranges and mounting locations.

Table 3.3

Sensors of SURALP

	Sensor	Number of Channels	Range
All joints	Incremental optic encoders	1 channel per joint	500 pulses/rev
Ankle	F/T sensor	6 channels per ankle	± 660 N (x, y-axes) ± 1980 N (z-axis) ± 60 Nm (all axes)
Foot	FSR	4 channels per foot	0 to 250 N
Torso	Accelerometer	3 channels	± 2 G
	Inclinometer	2 channels	± 30 deg
	Rate gyro	3 channels	± 150 deg/s
Wrist	F/T sensor	6 channels per wrist	± 65 N (x, y-axes) ± 200 N (z-axis) ± 5 Nm (all axes)
Head	CCD camera	2	640x480 pixels 30 fps

3.3. Controller Hardware

The control electronics is based on dSPACE modular hardware. A DS1005 microcontroller board of the dSPACE family is central controller in our hardware system. This is the board where all the reference generation and control algorithms explained in the following sections run. Apart from the μP, seven DS3001 incremental encoder input boards are used to provide the connectivity for 35 joint encoders. 31 of the connections provided by these incremental encoder boards are occupied with the joint encoders of the current design of SURALP. Two 32-inputs DS2002 Multi-Channel A/D Boards are employed for conversion of analog signals from inertial and force/torque sensors. One DS2103 Multi-Channel D/A Board provides 32 parallel D/A channels for the reference signals of the actuators. In addition to these, a DS4201-S Serial Interface Board provides 4 serial communication channels with selectable line transceivers (RS232, RS422 or RS485), which is set to RS232.

The rate gyro, accelerometer, inclinometer, FSR sensors and 6-axis force/torque sensors are integrated over the analog inputs. A Crossbow vertical gyro system, measuring 3 axis heading angles, accelerations and angular rates is connected to the DS4201-S Serial Interface Board and communicates via RS232. The analog outputs provide torque references for the four-quadrant Maxon & Faulhaber DC motor drivers. The controller and data acquisition boards mentioned above are housed by a dSPACE Tandem AutoBox enclosure, which is mounted in a backpack configuration in the robot assembly. The overall hardware structure is drawn in Figure 3.7. The rate gyro, accelerometer, inclinometer and Maxon & Faulhaber DC motor drivers are located in the torso of the humanoid robot. The power source and a remote user interface computer are placed externally. The CCD cameras are connected to the remote control PC via Firewire interfaces.

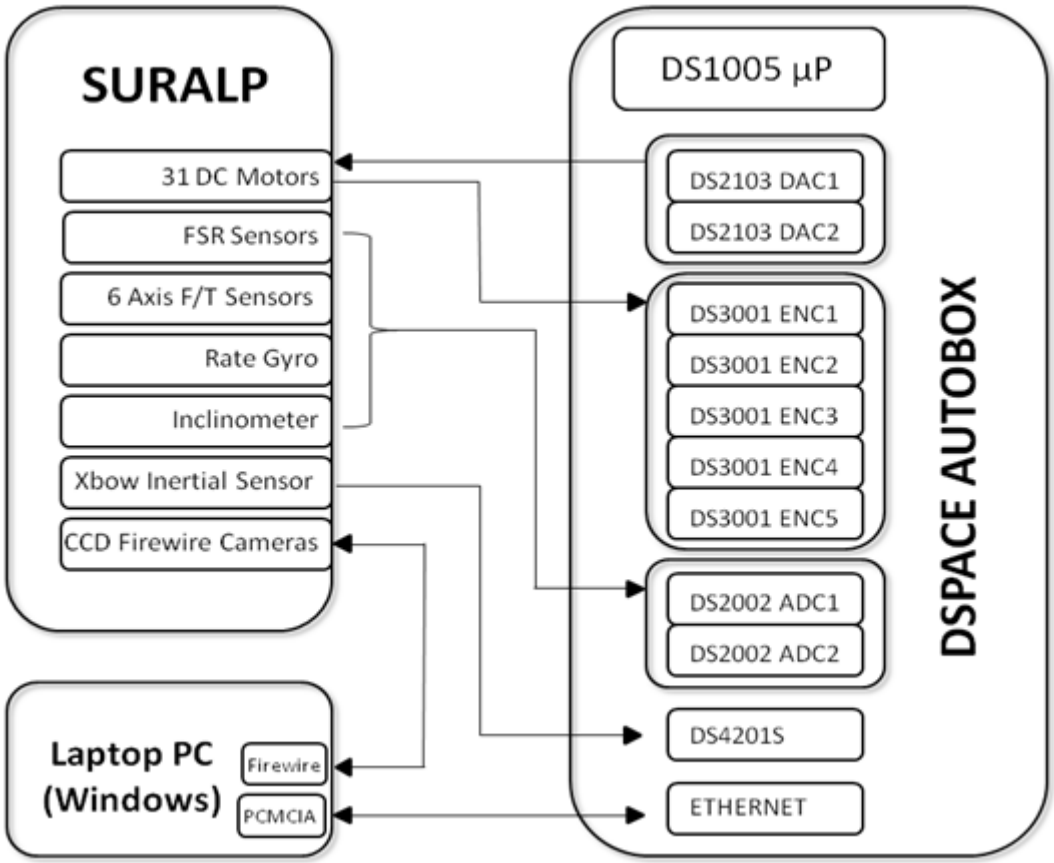

Figure 3.7 Overall hardware setup of the humanoid robot: SURALP

Chapter 4

4. WALKING TRAJECTORY GENERATION

4.1. Foot Reference Trajectory Generation

Various walking trajectory generation techniques used in the literature have been mentioned in Section 2.3. Similar to the studies [31], [32] and [35], in this thesis the reference x, y and z coordinates of foot centers with respect to the body center are generated as periodic functions of time completing the walking cycle (Figure 2.10). This periodic function approach is inspired by the works on the neural control of human locomotion, which consists of periodic solution with rhythms corresponding to the standard bipedal gaits [26].

The robot coordinate frames are shown in Figure 4.1. The foot position and orientations are expressed with respect to the body fixed coordinate system. In this thesis, the reference trajectories are generated as periodic functions of the x, y and z position references for coordinate frame centers attached to the two feet, with respect to a coordinate frame attached to the trunk of the biped robot. The trajectories are periodic and symmetric for both legs. Also it is assumed that the feet orientations are permanently parallel to the trunk. According to these reference positions of the feet, the joint trajectories are calculated using the inverse kinematics [47]. The details of the inverse kinematics used in this computation are included in Appendix A.

The foot trajectories in Cartesian x, y and z directions are computed as simple mathematical functions depending on a number of parameters. These continuous time-dependent functions are combinations of linear and sinusoidal functions and thus easy

to compute. Also, smoothing of these trajectories is possible at specific instants, such as landing or take-off instants of the feet.

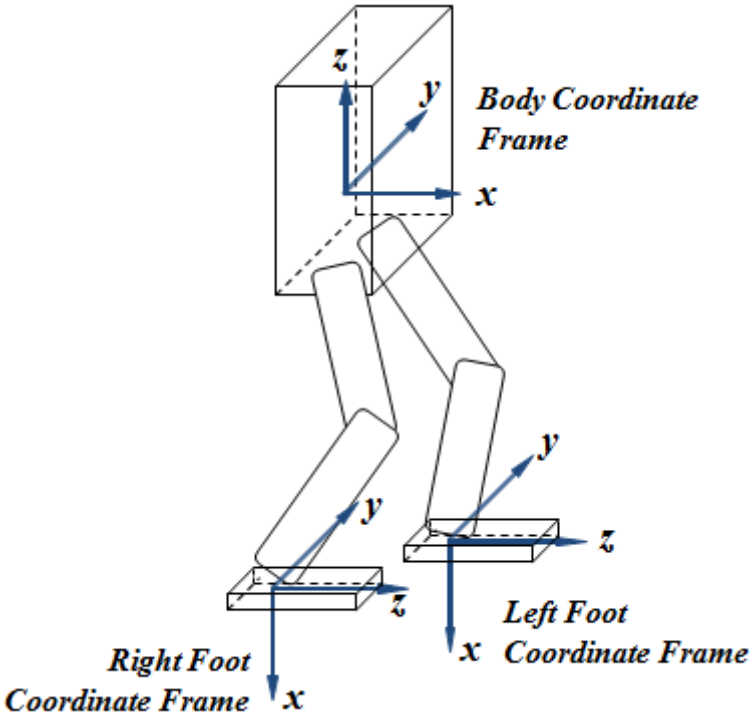

Figure 4.1 Coordinate frames of SURALP

The control structure of the robot SURALP enables the online adaptation of these parameterized trajectories. In addition to the online variations in the walking parameter values by user commands from the software, walking control algorithms enables the jump from one trajectory to another or online modifications on the reference trajectory curves in order to adapt to the walking environment. The flexibility of changing all the variables online provides an important opportunity in tuning the walking parameters without stopping the robot. In Figure 4.2, the layout used for parameter tuning and displaying the references is shown.

The reference trajectories consist of periodic repetition of walking phases for a determined time period (Figure 2.10). A step period is composed of the single support periods for right and left foot and two double support periods.

$$T_{step} = 2 \cdot (T_{ssp} + T_{dsp}) \tag{4.1}$$

The effective leg lengths; hip-to-sole distances of the legs, denoted by l_{right} and l_{left} respectively, are important parameters in trajectory generation. These parameters are independently used for compensation purposes described in the following chapter. Other walking parameters are explained in the corresponding sections.

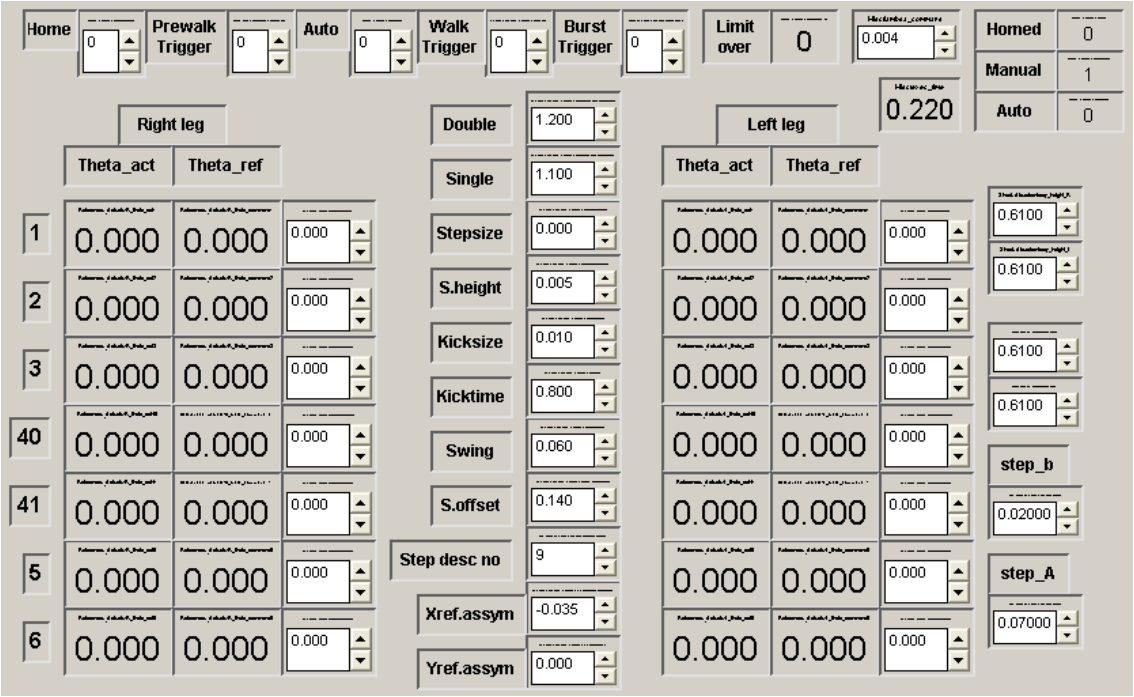

Figure 4.2 The user interface used in trajectory generation

Before starting to walk, the robot needs to be set to its pre-walk configuration. This is the configuration of the robot where the joint trajectories are set to their initial values at $t = 0$. In the pre-walk position, the distance between the feet is determined by the swing offset parameter and knee joints are bent such that the effective lengths are at their initial values (Table 4.1). The reason of this bending is to avoid singularity while computing the inverse kinematics of the legs.

$$l_{right} = l_{left} = 0.62\ m \tag{4.2}$$

4.1.1. Foot Trajectory Generation in the x-Direction

The Cartesian *x*-direction trajectories of the feet are composed of double support and single support phases. The feet move forward and backward with respect to the body coordinate frame. In the double support phase, the *x* references of the feet are kept constant, whereas in the single support phase, the references of both support and the swing foot followed a cosine function in opposite direction and symmetric to each other by a magnitude of the step-size parameter. The *x*-direction trajectory expressed in the body coordinate frame is computed as the following;

$$x_{ref}=\begin{cases}0.5\cdot d_{step} & if\ \ 0\le t<0.5\cdot(T_{dsp}+T_{push})\\ 0.5\cdot d_{step}\cdot\cos\left(\pi\dfrac{t-0.5\cdot T_{dsp}-0.5\cdot T_{push}}{T_{ssp}-0.5\cdot T_{push}}\right) & 0.5\cdot(T_{dsp}+T_{push})\le t<0.5\cdot T_{dsp}+T_{ssp}\\ -0.5\cdot d_{step} & 0.5\cdot T_{dsp}+T_{ssp}\le t<1.5\cdot T_{dsp}+T_{ssp}+0.5\cdot T_{push}\\ -0.5\cdot d_{step}\cdot\cos\left(\pi\dfrac{t-1.5\cdot T_{dsp}-T_{ssp}-0.5\cdot T_{push}}{T_{ssp}-0.5\cdot T_{push}}\right) & 1.5\cdot T_{dsp}+T_{ssp}+0.5\cdot T_{push}\le t<1.5\cdot T_{dsp}+2\cdot T_{push}\\ 0.5\cdot d_{step} & 1.5\cdot T_{dsp}+2\cdot T_{push}\le t\end{cases} \quad (4.3)$$

Using an offset parameter called the *x*-reference asymmetry, which determines the average position of the feet in *x*-direction with respect to the body coordinate frame, the *x* references for right and left legs are obtained as in (4.4) and (4.5).

$$x_{ref}^{right}=x_{ref}+x_{ref\_asymmetry} \quad (4.4)$$

$$x_{ref}^{left}=-x_{ref}+x_{ref\_asymmetry} \quad (4.5)$$

The *x*-direction trajectories computed are shown in Figure 4.3.

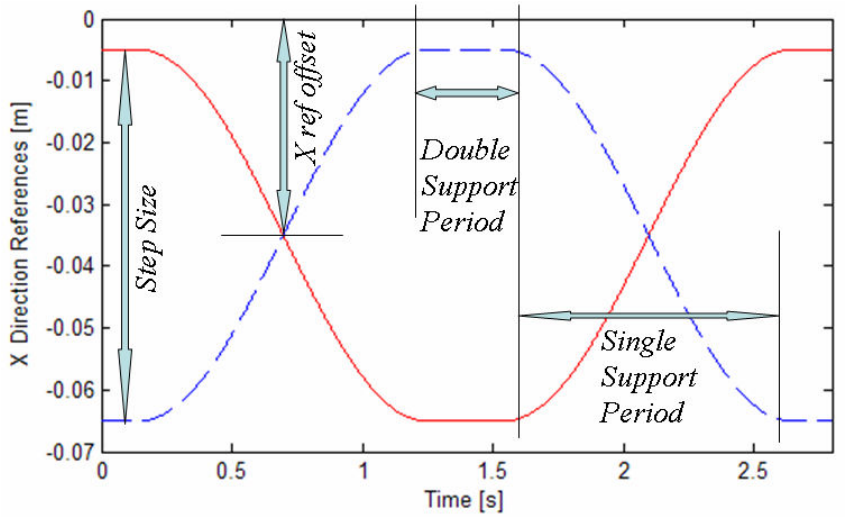

Figure 4.3 Typical *x*-direction Cartesian reference trajectories (solid: right, dashed: left)

4.1.2. Foot Trajectory Generation in the y-Direction

The robot is required to swing in *y*-direction with the aim of lifting the swing foot and keeping the balance [34]. The swinging of the robot is in the opposite direction of the *y*-direction foot references because the support foot is in contact with the ground.

Additionally, to increase the stability of the walk, the peaks of the swing curves are softened using a delay period, in which the references are kept constant. The computation of this trajectory as expressed in the body coordinate frame using sinusoidal functions is as in the following;

$$y_{ref} = \begin{cases} d_{swing} \cdot \sin\left(\pi \dfrac{t}{T_{dsp}+T_{ssp}-T_{delay}}\right) & if\ \ 0 \le t < 0.5\cdot(T_{dsp}+T_{ssp}-T_{delay}) \\ d_{swing} & 0.5\cdot(T_{dsp}+T_{ssp}-T_{delay}) \le t < 0.5\cdot(T_{dsp}+T_{ssp}+T_{delay}) \\ d_{swing} \cdot \sin\left(\pi \dfrac{t-T_{delay}}{T_{dsp}+T_{ssp}-T_{delay}}\right) & 0.5\cdot(T_{dsp}+T_{ssp}+T_{delay}) \le t < 1.5\cdot T_{dsp}+1.5\cdot T_{ssp}-0.5\cdot T_{delay} \\ -d_{swing} & 1.5\cdot T_{dsp}+1.5\cdot T_{ssp}-0.5\cdot T_{delay} \le t < 1.5\cdot T_{dsp}+1.5\cdot T_{ssp}+0.5\cdot T_{delay} \\ d_{swing} \cdot \sin\left(\pi \dfrac{t-2\cdot T_{delay}}{T_{dsp}+T_{ssp}-T_{delay}}\right) & 1.5\cdot T_{dsp}+1.5\cdot T_{ssp}+0.5\cdot T_{delay} \le t \end{cases} \quad (4.6)$$

Shifting the y_{ref} via the variables *y*-reference asymmetry, which determines the average position of the feet in *y*-direction with respect to the body coordinate frame, and the swing offset, the *y* references for right and left legs are obtained as in (4.7) and (4.8).

$$y_{ref}^{right} = y_{ref} + y_{ref\_asymmetry} - d_{swing\_offset} \quad (4.7)$$

$$y_{ref}^{left} = y_{ref} + y_{ref\_asymmetry} + d_{swing\_offset} \quad (4.8)$$

The *y*-direction trajectories computed are shown in Figure 4.4.

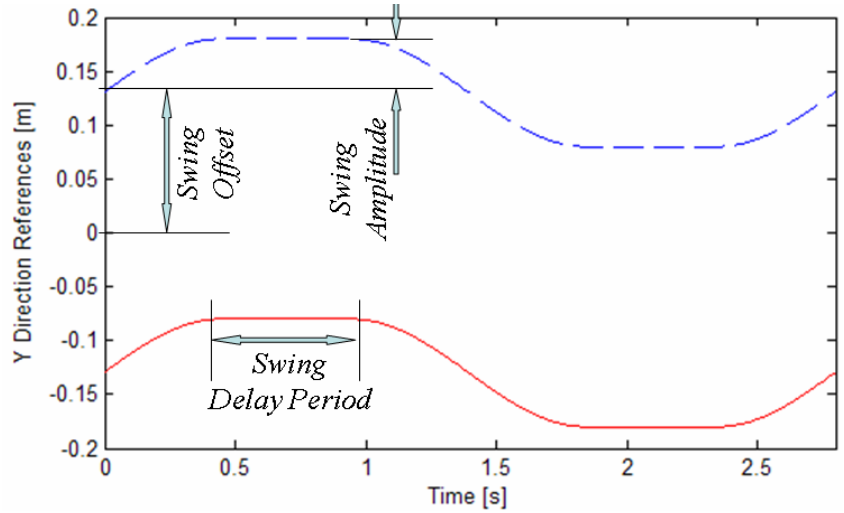

Figure 4.4 Typical *y*-direction Cartesian reference trajectories (solid: right, dashed: left)

4.1.3. Foot Trajectory Generation in the z-Direction

The robot needs to lift its feet upwards to take a step. The *z*-direction reference trajectories are negative, because they are expressed in the body fixed coordinate frame. Although the magnitudes of the *z* references are equal for both right and left legs, their timing has a shift due to the fact that only the swing foot will be lifted. At the beginning and the end of the swing phases, *z*-direction references are zero and the peaks of *z* references are reached after the middle of the swing phases.

In addition to the take-off of the feet, this thesis introduces the pushing the ground approach in *z*-direction trajectory generation. In this approach, the ground is pushed by the feet before the take off for a determined period of time with the parameter called ground push period. Thus, the trajectory is divided into 5 phases. The first and the last phases are the beginning and the end of the swing phase, where the magnitude is zero. The other three phases are;

- ground push phase with a "1-cosine" function in order to smooth and reduce the impact generated by the pushing,
- foot rise phase, again with a "1-cosine" function,
- foot landing phase from the step height to zero with a "cosine" function for soft landing.

The *z*-direction trajectories for the left foot are computed as the following;

$$z_{ref}^{right}=\begin{cases} 0 & if\ \ 0\le t<0.5\cdot T_{dsp} \\ 0.5\cdot h_{push}\cdot\left(1-\cos\left(2\pi\dfrac{t-0.5\cdot T_{dsp}}{T_{push}}\right)\right) & 0.5\cdot T_{dsp}\le t<0.5\cdot(T_{dsp}+T_{push}) \\ -h_{push}+0.5\cdot(h_{push}+h_{step})\cdot\left(1-\cos\left(2\pi\dfrac{t-0.5\cdot(T_{dsp}+T_{push})}{T_{ssp}}\right)\right) & 0.5\cdot(T_{dsp}+T_{delay})\le t<0.5\cdot(T_{dsp}+T_{ssp}+T_{push}) \\ 0.5\cdot h_{step}\left(1+\cos\left(2\pi\dfrac{t-0.5\cdot(T_{dsp}+T_{ssp}+T_{push})}{T_{ssp}-T_{push}}\right)\right) & 0.5\cdot(T_{dsp}+T_{ssp}+T_{push})\le t<0.5\cdot T_{dsp}+T_{ssp} \\ 0 & 0.5\cdot T_{dsp}+T_{ssp}\le t \end{cases} \quad (4.9)$$

Unlike the *x* and *y* references, *z* trajectories are not symmetric in timing and there is a time shift in the references. Thus, the *z* references for the right leg is computed similar to (4.9) but with different time specifications. Applying the effective leg lengths l_{right} and l_{left}, Cartesian foot references in *z*-direction are obtained (Figure 4.5).

$$z_{ref}^{right} = -l_{right} + z_{ref} \tag{4.10}$$

$$z_{ref}^{left} = -l_{left} + z_{ref} \tag{4.11}$$

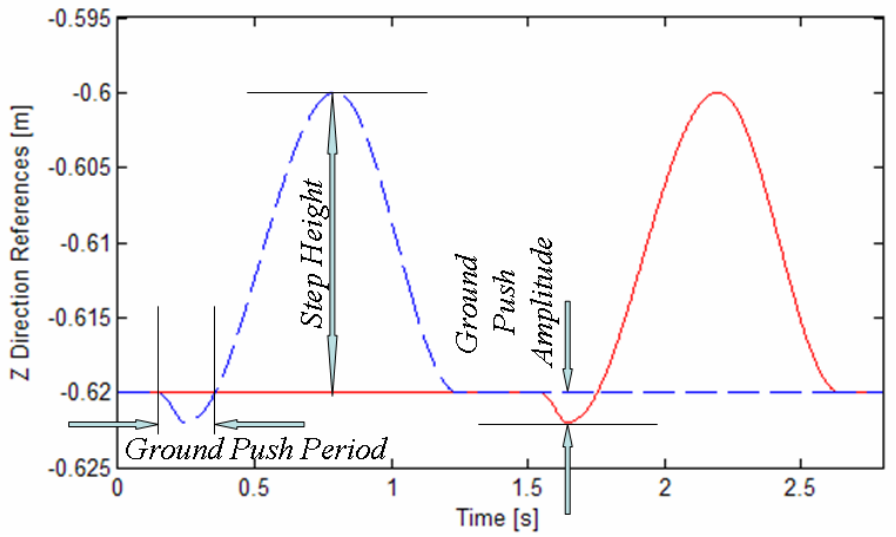

Figure 4.5 *z*-direction Cartesian reference trajectories (solid: right, dashed: left)

The walking pattern of the robot is generated by the synchronous run of these trajectories in *x*, *y* and *z*-directions. Typical walking parameters used in the experiments of this thesis are given in Table 4.1.

Table 4.1

Trajectory generation parameters

Single support period	1.2 s
Double support period	1.1 s
Ground push period	0.8 s
Swing delay period	0.5 s
Step period	4.6 s
Step height	1.5 cm
Body pitch angle	3 deg
Step size	6 cm
Ground push amplitude	1 cm
Swing amplitude	6.5 cm
Swing offset	14 cm
Body height	62 cm
Initial *x*-reference offset	-3.5cm

4.2. Upper Body Trajectory Generation

4.2.1 Waist and Arm Swing Reference Trajectories

Due to the angular momentum created by the swinging leg, a yaw moment is generated at the supporting foot while walking. Up to an amount, this moment is compensated by the friction between the floor and the supporting foot [33]. This moment needs to be compensated in order to prevent sliding of the supporting foot and turning of the robot around the yaw axis. By generating waist and arm swing trajectories, the sliding effect of the yaw moment can be decreased. The waist axis reference has a similar form to the x-direction foot references shown in Figure 4.3.

The arms of the robot have given an initial angle of 30 degrees in the shoulder and the elbow in the opposite direction, so that the arms have a human-like walking configuration (Figure 3.2). In addition to the generation of waist trajectories to counteract the angular momentum, the arms can also be used with the same purpose.

4.2.2 Body Pitch Angle Reference

The foot orientation references used in the inverse kinematics are fixed and they are computed such that the feet are parallel to the ground. However, the robot body is oriented with a small pitch angle (3 degrees) with respect to the ground, which is also referred as pitch tilt angle. By the virtue of the body pitch tilt angle, the robot center of mass is moved forward from the behind of the waist axis, closer to the center of the pelvis.

Chapter 5

5. WALKING CONTROL ALGORITHMS

Even though a smooth reference trajectory is generated as described in the previous chapter, to realize a robust walk and maintain the balance of the robot, balance control algorithms are required. In order to cope with disturbances, inclination or unevenness of the walking environment, various control techniques have been employed using sensory feedback, similar to the ones published in [48]. Figure 5.1 shows the control algorithms employed and the sensors used for them in a block diagram. Scheduling and the working principles of these controllers are explained in the following section. Experimental results with the controllers described in this chapter are presented in Chapter 6.

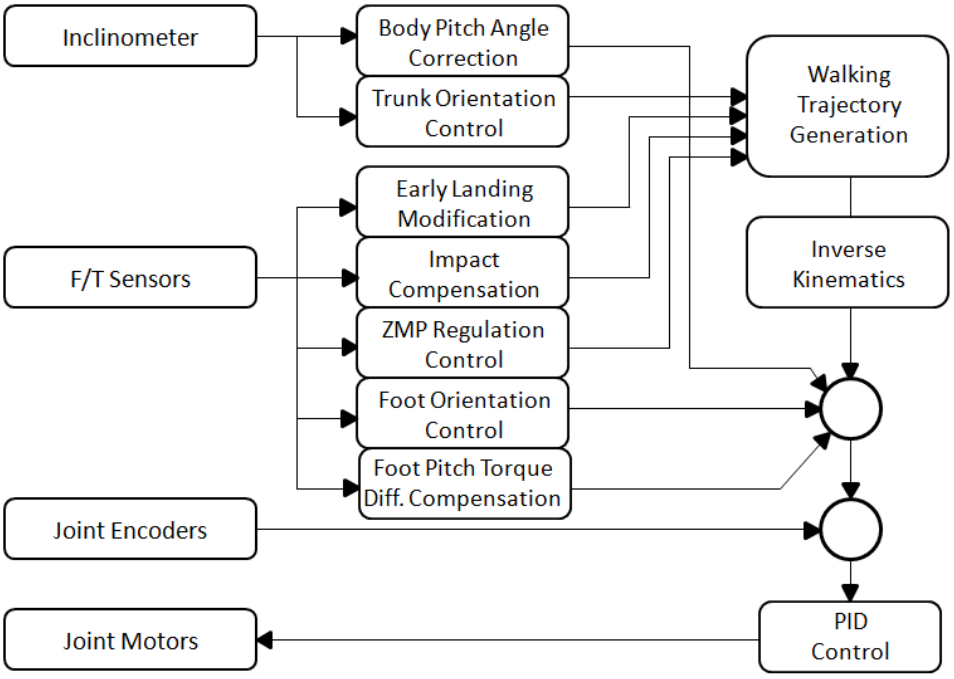

Figure 5.1 The overall control block diagram of SURALP

5.1. Independent Joint Control

Reading motor angular position from the incremental encoders, the reference tracking performance of each joint with sinusoidal references is tested and PID control gains are tuned via trial and error. A second, final tuning is carried out during walking. In order to achieve a stable walk, it is significant that all joints follow the reference trajectories with a fast response time, limited steady state error, oscillation and overshoot. The trajectories are tracked very successfully with peak position errors corresponding to a few encoder pulses, with a sampling rate of 1 kHz. The PID control gains are given in the following table.

Table 5.1

PID control parameters

	K_p	K_d	K_i
Hip-Yaw	12000	30	60
Hip-Roll	150000	30	200
Hip-Pitch	30000	30	80
Knee 1-2	30000	50	50
Ankle-Pitch	100000	60	100
Ankle-Roll	100000	60	80
Shoulder Roll-1	20000	50	80
Shoulder Pitch	20000	50	80
Shoulder Roll-2	20000	10	30
Elbow	20000	10	20
Wrist Roll	1000	10	10
Wrist Pitch	5000	10	20
Neck Pan	20000	10	30
Neck Tilt	5000	10	20
Waist	20000	50	80

5.2. Home Posture Adjustment Control Algorithms

Our experiments indicate that the home posture of the robot has a very significant effect on the stability of the walk. Since the Maxon DC motors used in SURALP have incremental encoders mounted on them, the position counters are cleared after turning off the power of the controllers and a zeroing process is necessary before the next experimental work. Since a perfect manual zeroing of joint positions is quite hard for a 29 D.O.F. humanoid robot, inaccuracies will occur in the initial home posture, which need to be compensated. In this thesis, an automatic homing routine is proposed.

The automatic homing routine aims equal weight distribution on the two feet and a straight body upper posture in both roll and pitch axes. Control algorithms for the adjustment of the home posture use sensory information from 6-axis force/torque sensors at the ankles and an inclinometer mounted on the trunk. Inspired by the idea of [49], four algorithms are applied simultaneously during the homing process: Foot pitch torque difference compensation, ZMP regulation foot orientation control and trunk orientation control.

The homing starts with a rough manual homing process with position increments of 0.5 degrees commanded from the graphical user interface. At the end of the manual homing, the pre-walk pose of the robot (mentioned in Section 4.1) is commanded. Then, the robot is lowered to the ground and is ready to the activation of automatic homing algorithms. With the use of these techniques, the robot adapts to the ground conditions and the offset values due to the inaccuracies in initial home posture are captured. These offset values are then applied before the experiments.

5.2.1 ZMP Regulation

The ZMP criterion is an important measure of stability in bipedal walk. The ZMP should be inside the supporting polygon of the two feet in the double support phase and inside the supporting sole area in the single support phases. A ZMP regulation is proposed for the automatic homing process of the humanoid robot [49]. For this purpose, a simple proportional action relation between the ZMP error and pelvis horizontal position proved to be successful. The ZMP reference for zeroing the robot is defined in the middle of the supporting polygon as in Figure 5.2.

$$\overline{X}_{ref\ offset}(s) = X_{ref\ offset}(s) + K_{P-ZMP\ X}(X_{ZMP\ desired}(s) - X_{ZMP\ actual}(s)) \quad (5.1)$$

$$\overline{Y}_{ref\ offset}(s) = Y_{ref\ offset}(s) + K_{P-ZMP\ Y}(Y_{ZMP\ desired}(s) - Y_{ZMP\ actual}(s)) \quad (5.2)$$

$X_{ref\ offset}$ and $Y_{ref\ offset}$ are set to the center locations of the Cartesian reference trajectories shown in Figure 5.2. $\overline{X}_{ref\ offset}$ and $\overline{Y}_{ref\ offset}$ are modified by the control method. In order to shift the real ZMP to the desired value, which is the ZMP reference shown in Figure 5.2, the robot center of gravity is shifted in *x* and *y* axes by adding the offset values to $x_{ref\_asymmetry}$ and $y_{ref\_asymmetry}$ explained in Section 4.1.

$$x_{ref\_asymmetry} = x_{ref\_asymmetry} + \overline{X}_{ref\ offset}(s)) \quad (5.3)$$

$$y_{ref\_asymmetry} = y_{ref\_asymmetry} + \overline{Y}_{ref\ offset}(s)) \quad (5.4)$$

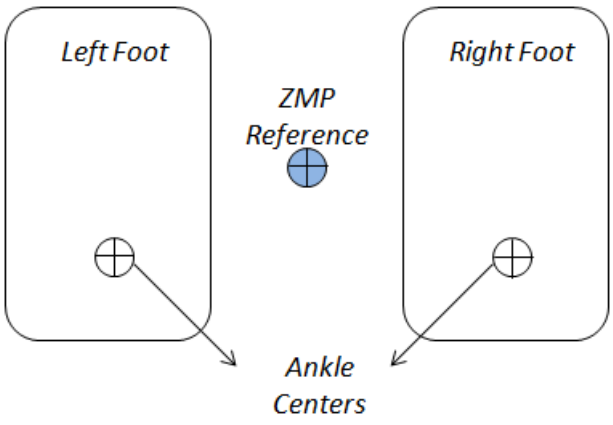

Figure 5.2 The ZMP reference for robot zeroing

5.2.2 Foot Orientation Control

This approach aims the adaptation of both feet to the ground by modifying the planned ankle joint angles. The scheme computes joint angle reference modifications in such a way that the feet are aligned parallel to the walking surface when they are in contact with the ground. This case is shown in Figure 5.3 from the frontal plane.

The reference modification law is in the form of a first order filter applied on the foot to ground contact torques. For the roll axis of the ankle, the following reference modification law is employed:

$$\bar{\theta}_{roll}(s) = \theta_{roll}(s) + \frac{K_{roll}}{s + \lambda_{roll}} T_{roll}(s) \tag{5.5}$$

where s is the Laplace variable. θ_{roll} is the roll joint reference angle computed from the inverse kinematics. $\bar{\theta}_{roll}$ is the reference angle after the reference modification. T_{roll} is the torque about the roll axis due to the interaction of the foot with the ground. T_{roll} is measured by torque sensors positioned at the ankle. K_{roll} and λ_{roll} are low pass filter constants which are determined by trial and error in our approach.

In the digital implementation, the Laplace domain transfer function in (5.5) is approximated by a difference equation using Tustin's approximation.

In the homing of the robot, when the foot is in contact with the ground only with a corner or an edge, a torque is developed and with the application of (5.5), the joint angle references are modified in such a way to turn the ankle to achieve foot orientation parallel to the ground. This modification law is applied to the two legs independently.

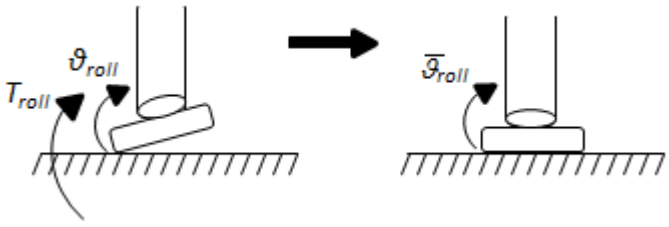

Figure 5.3 Simple model for the foot orientation control

5.2.3 Trunk Orientation Control

The inclination of the robot body (or trunk) is an important indicator of the stability of the walk. In the homing process, due to imperfect manual initialization of joints and uneven ground conditions, the robot trunk needs to be aligned straight in both frontal and sagittal planes. Inspired by the idea [7] to keep the trunk vertically aligned on uneven ground conditions, the effective leg lengths and ankle pitch/roll angles are controlled simultaneously. In the sagittal direction part of this controller the ankle pitch angles are modified by using feedback from body inclination, where the information from the inclinometer is used (Figure 5.4 and 5.5). The control law employed is

$$\bar{\theta}_{pitch}(s) = \theta_{pitch}(s) + \left(K_{P-pitch} + K_{I-pitch} \frac{1}{s} \right) \theta_{trunk\ pitch}(s) \tag{5.6}$$

where $\theta_{pitch}(s)$ is the pre-planned pitch angle reference for the ankle joints (for the right ankle and the left ankle) and $\bar{\theta}_{pitch}(s)$ is the modified reference. $\theta_{trunk\ pitch}(s)$ is the trunk pitch angle measured by the inclinometer. $K_{P-pitch}$ and $K_{I-pitch}$ are the trunk pitch control proportional and integral action gains, respectively. In the lateral direction, for the ankle roll joints, the landing foot orientation controller described above in this section is employed. The trunk roll angle control is carried out by using the effective leg lengths which in our study are defined as the distances between the hip joints and foot soles. The feedback law which uses the inclinometer roll angle measurement is as follows.

$$\bar{l}_{left}(s) = l_{left}(s) + \left(K_{P-roll} + K_{I-roll} \frac{1}{s} \right) \theta_{trunk\ roll}(s) \tag{5.7}$$

$$\bar{l}_{right}(s) = l_{right}(s) - \left(K_{P-roll} + K_{I-roll} \frac{1}{s} \right) \theta_{trunk\ roll}(s) \tag{5.8}$$

In these expressions, l_{left} and l_{right} are the pre-planned effective lengths of the left and right leg, respectively. $\bar{l}_{left}$ and $\bar{l}_{right}$ are their versions after the application of the trunk orientation controller. K_{P-roll}, K_{I-roll}, K_{P-roll} and K_{I-roll} are controller gains and $\theta_{trunk\ roll}$ is the measured trunk roll angle.

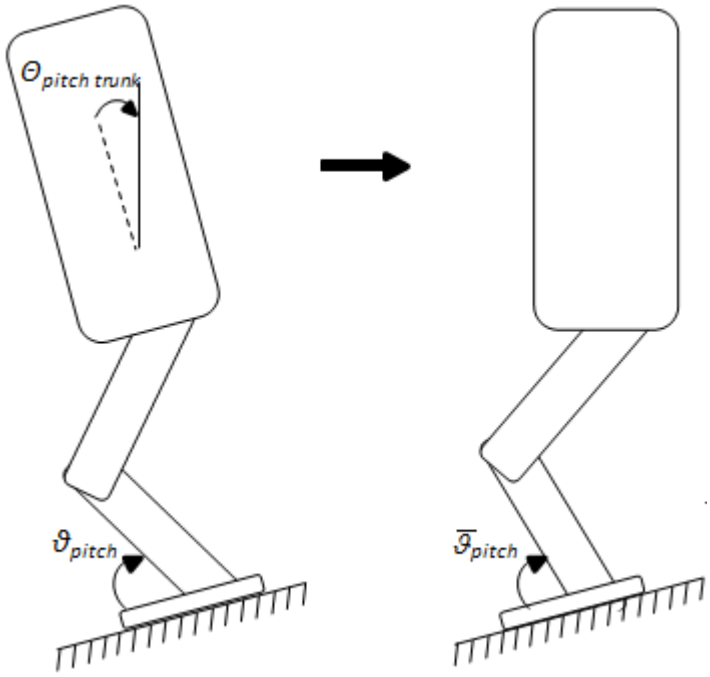

Figure 5.4 Simple model for the trunk orientation control (pitch axis)

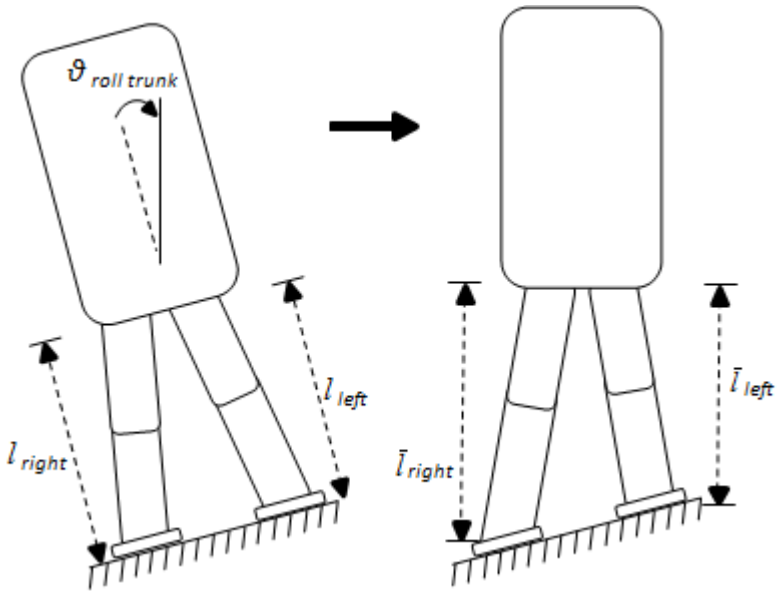

Figure 5.5 Simple model for the trunk orientation control (roll axis)

5.2.4 Foot Pitch Torque Difference Compensation

The ankle pitch control action for the regulation of trunk orientation is applied on the two ankles simultaneously. However, the ground irregularities or the difference between the initial values in the joint zeroing process of the two ankle pitch angles can cause the two feet make different angles with the ground surface, which will generate different torque values on the ankles. In such a case, typically the toe or heel parts of the feet will be off ground causing unstable behavior and large magnitude fluctuations in body inclination angles. In order to align both feet parallel to the ground, a torque difference compensator is proposed, which makes the ankle torques equal. This approach is applied for our biped robot as a PI controller;

$$\theta_{difference}(s) = \left(K_{P-difference} + K_{I-difference} \frac{1}{s} \right) \left(T_{pitch\ \ right}(s) - T_{pitch\ \ left}(s) \right) \tag{5.9}$$

$$\overline{\theta}_{pitch\ \ right}(s) = \theta_{pitch}(s) + \theta_{difference}(s) \tag{5.10}$$

$$\overline{\theta}_{pitch\ \ left}(s) = \theta_{pitch}(s) - \theta_{difference}(s) \tag{5.11}$$

In (5.9), $T_{pitch\ left}$ and $T_{pitch\ right}$ are the ankle pitch torques measured by the 6-axis force/torque sensors. The application of the controller is by superposition with the trunk orientation control which also acts on the ankle pitch angles.

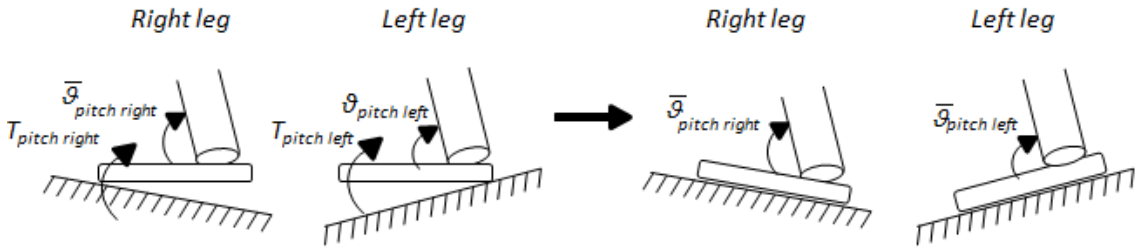

Figure 5.6 Simple model for the foot pitch torque difference compensation

5.3. Walking Balance Control Algorithms

Stable trajectory generation may not be sufficient to realize the maintenance of the balance during the walk in cases of external disturbances and inclined or uneven ground conditions. After a successful homing process, online balance control algorithms are applied during the walk. The foot and trunk orientation controllers explained in the previous section (Section 5.2) are employed in walking experiments too.

As explained in 5.2.2, the foot orientation control is based on the difference between the actual and the planned angle of the swing foot. During the walk, the function of this approach is to adapt the landing foot to the ground with a soft and smooth landing. The joint angle reference modifications are computed same as (5.5). Using the reaction torque developed when the landing foot is not perfectly parallel to the ground, the ankle joint angle references are modified to achieve a flat foot orientation.

As described in 5.2.3, the trunk orientation control is an important tool for keeping the robot torso in an upright position. With the same objective, a similar balance control algorithm is developed for the walking. This method is called body pitch angle correction and designed for fast response during the walk. This controller modifies the ankle pitch angles by using the feedback obtained from the inclinometer.

In addition to the methods 5.2.2, the following balance control techniques, including the body pitch angle correction, ground impact compensation and early landing compensation are introduced for a stable walk.

5.3.1 Body Pitch Angle Correction

With the aim of keeping the robot torso aligned in the sagittal plane with an angle determined by the control designer and reducing the oscillations around the pitch axis, an angle correction algorithm similar to the one in 5.2.3 is developed for the walking of the robot. Different from the algorithm developed for the automatic homing process, a faster response is required to modify the body pitch angle of the robot. The

control action must be fast enough to follow the pitch oscillations and compensate them during the walk. Furthermore, the robot is aimed to be aligned with an angle determined by the pitch tilt reference explained in Section 4.2, rather than aligning the torso strictly straight. This controller modifies the ankle pitch angles by using the feedback obtained from the inclinometer (Figure 5.4). The control law employed is:

$$\bar{\theta}_{pitch}(s) = \theta_{pitch}(s) + \left(K_{P-pitch} + K_{I-pitch}\frac{1}{s} \right)\left(\theta_{trunk\ pitch}(s) - \theta_{pitch\ tilt} \right) \tag{5.12}$$

where $\theta_{pitch}(s)$ is the pre-planned pitch angle reference for the right and left ankle joints and $\bar{\theta}_{pitch}(s)$ is the modified reference. $\theta_{trunk\ pitch}(s)$ is the trunk pitch angle measured by the inclinometer and $\theta_{pitch\ tilt}(s)$ is the pitch tilt angle reference. $K_{P-pitch}$ and $K_{I-pitch}$ are the trunk pitch control proportional and integral action gains, respectively.

In order to adapt the trunk orientation control in the homing process to the online walking control algorithms, the control parameters $K_{P-pitch}$ and $K_{I-pitch}$ are tuned again. The same control action is applied to both right and left ankle pitch angles. This online pitch angle modification is employed only in the double support phase of the walking, where both feet are landed on the ground.

5.3.2 Ground Impact Compensation

Another important problem in achieving stable walking is the impact generated at the landing of the swing foot. Even a small tilting of the robot upper body to the front will cause the swing foot land early and the leg will try to push the ground. Due to the ground interaction force acting on the landing foot due to the impact, the robot will vibrate and this will affect the stability of the walk in each step. In order to compensate this impact, a virtual mass-spring-damper system is positioned between the hip and ankle. Using the vertical force data from the force/torque sensors at the ankles, the distance between the hip and sole of the landing foot is modified by the following second order relation:

$$\bar{l}(s) = l(s) - \frac{1}{m_l s^2 + b_l s + k_l} F_z(s) \tag{5.13}$$

In (5.13) l represents the effective length reference obtained from Cartesian foot reference trajectories. $\bar{l}$ is the modified version of the distance after the compensation. F_z is the z direction component of the ground interaction force acting on the foot measured by the force/torque sensors. m_l, b_l and k_l are the desired mass, damping and stiffness parameters of the mechanical admittance relation described in (5.13), which are tuned as a critically damped system. The ground impact compensation is triggered with any landing of the foot, not just for the early landing. It is deactivated after a certain time specified by the control designer, where in these experiments 0.4 seconds is assigned as the activation time. It is important to note that, the height between the hip and sole is no more equal to its original value after this compensation. In order to return the effective length to its original reference value, at the end of the impact compensation phase the following equation is applied:

$$\bar{l}(t) = l(t) - 0.5(l(t_0) - \bar{l}(t_0))\left(1 + \cos((t - t_0)\omega_{return}\right) \tag{5.14}$$

where t_0 is the time at the end of the impact compensation phase and ω_{return} determines the speed of return of $\bar{l}$ to l. By (5.14), beginning with the final $\bar{l}$ value of the impact compensation phase, $\bar{l}$ returns to the original reference value l after a smooth transient behavior. The test results showed that it is better to apply this modification law to the two legs independently.

As in the case of other techniques, Tustin's approximation of the continuous relation is obtained and applied.

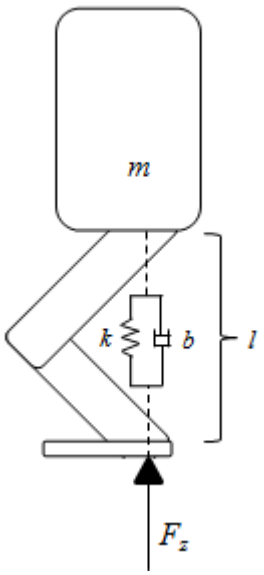

Figure 5.7 Simple model for the ground impact compensation

5.3.3 Early Landing Modification

The walking phases and the reference trajectories are explained in the following chapters, including the takeoff and landing timing for both right and left feet in *z*-direction. Any disturbance or ground irregularity and the inclination of the robot trunk might result in a difference in the landing timing of the swinging foot from the ideal reference timing. So, in addition to the planned timing captured from the reference curves, real foot landing timings must be determined based on the ground reaction force exerted on the ankles. If the swing foot lands before the prescribed landing time, which is generally the case, this landing is called an early landing. This situation is captured when the force/torque sensors at the ankles read a force value larger than a determined threshold value in the landing phase of the swing foot.

One of the main problems of early landing of a swung foot is that when it lands to the ground before the beginning of the double support phase as expected, it will go on moving forward following the planned reference curve. When the *x*-direction foot references shown in Figure 4.3 are investigated, it is observed that the supporting foot will move backward in the body coordinate system at the same time. Therefore, right after an early landing the feet on the ground will try to push the robot in two different directions. The feet will slip, the robot will turn, and the trunk will significantly oscillate. In order to avoid such a condition, the *x*-direction references for both right and left feet are modified in the case of an early landing. The modification is developed for two kinds of trajectory generation methods. The first one is developed for the parametric function based reference trajectories applied in this thesis, where the *x*-direction references for right and left feet are symmetric and parallel. The second one is adapted for ZMP based trajectories, where the *x*-direction references are not completely symmetric [50].

5.3.3.1 Early Landing Modification for Function Based Trajectories

In this case, the timing and the magnitudes of the step size for the right and left feet are completely the same. Specifically, this modification "stops" the *x*-direction references of the feet at their values they had at the instant of early landing, as shown in Figure 5.8. The *x* references for both feet are kept fixed until the next walking cycle and continue from their fixed values, whenever the planned *x* direction references reach the captured value again.

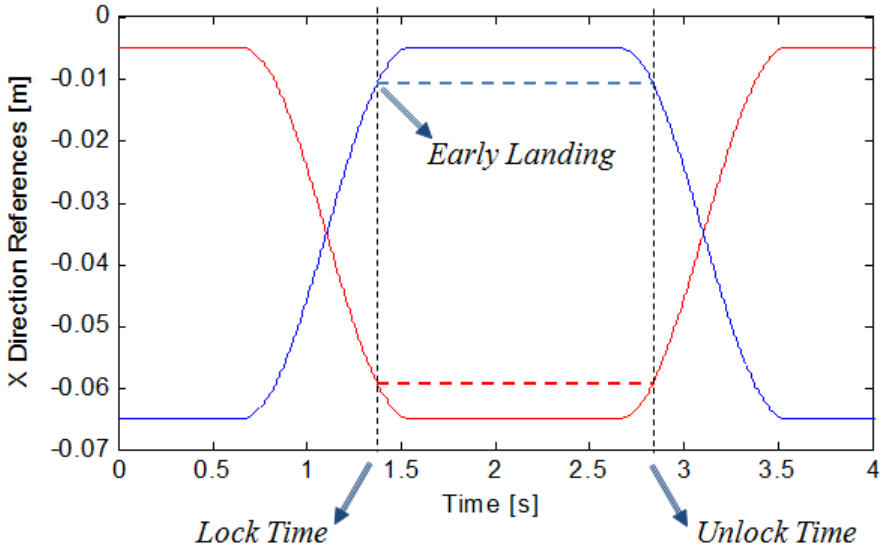

Figure 5.8 Early landing modification for symmetric *x*-direction references

5.3.3.2 Early Landing Modification for ZMP Based Trajectories

Different from the previous case, in ZMP based trajectories the *x* direction reference curves are not symmetric due to differences in the timing and step sizes. Thus, a more complex solution is required for this case. When the *x* direction references for the ZMP based trajectories are investigated, it can be seen that the previous solution cannot be applied for this case. If the *x* reference values of both feet are kept at the instant of early landing, the supporting foot will not reach its planned *x* references when

the landed foot reference reaches its planned value. So, this will result in a jump in the reference of the supporting foot and the robot will hop and vibrate seriously.

In order to solve this problem and adapt the early landing modification method to asymmetric *x*-direction references, a parallelogram method is developed. Instead of fixing the reference at the instant of the early landing, using the landing time and the reference value at that instant, the lock time, unlock time and the unlock values are computed for both swing and support foot. The new restricted references are formed by combining these values in a parallelogram. At the final step, the reference values are kept constant at the instant of landing. Since the references are parallel in the body coordinate frame, in the case of an early landing the feet will not further move and the unexpected turning and oscillations of the robot will be avoided.

Figure 5.9 shows an experimental result of walking based on ZMP trajectories. The solid curves are the original *x*-direction ZMP foot references and the dotted curves are their modified versions.

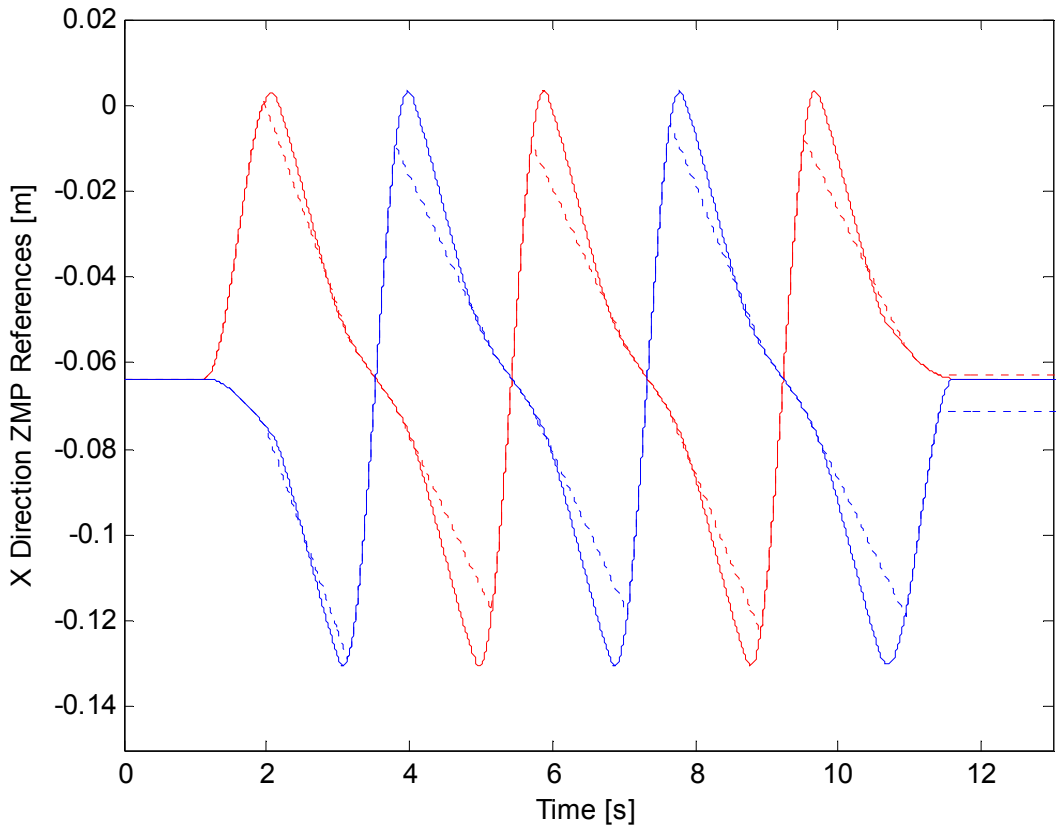

Figure 5.9 Early landing modification for asymmetric *x*-direction references (red: right and blue: left, solid: original, dotted: modified)

Chapter 6

6. EXPERIMENTAL RESULTS

6.1. Automatic Homing Results

The controllers discussed in Section 5.2 are employed for the automatic homing process of the robot. To realize the success of the controllers, the adaptation of the robot to an inclined plane is tested (Figure 6.1). The homing algorithms are applied one by one in order to show their control effects clearly.

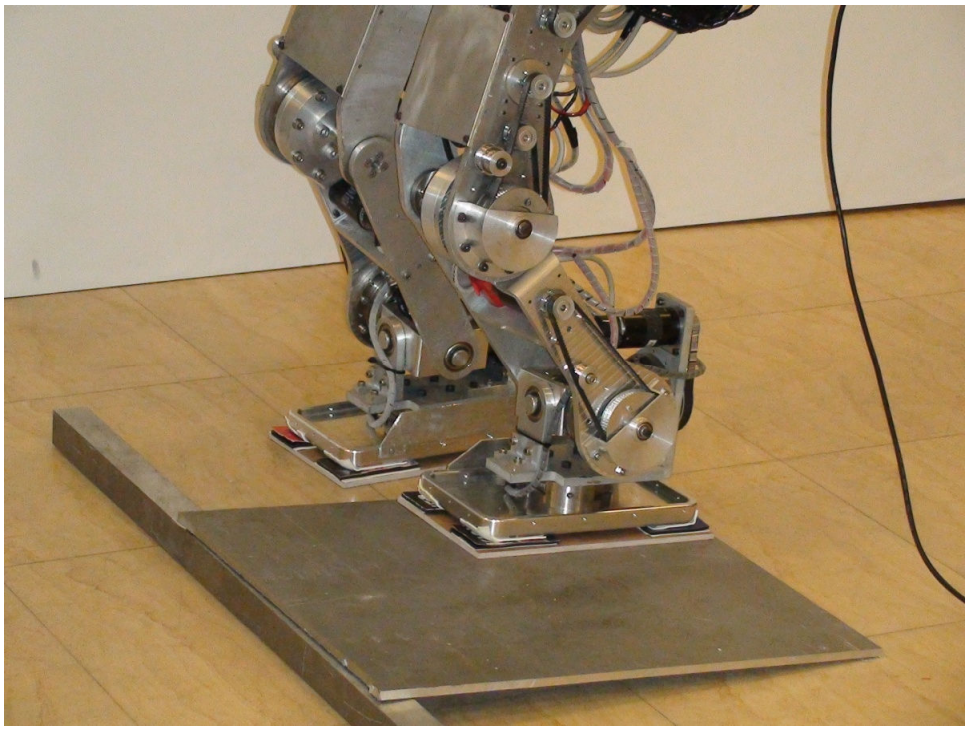

Figure 6.1 Inclined plane used in the automatic homing process

Figure 6.2 shows the ankle roll angle modification in the homing process. The control technique modified the ankle joints so that both feet are parallel to the ground.

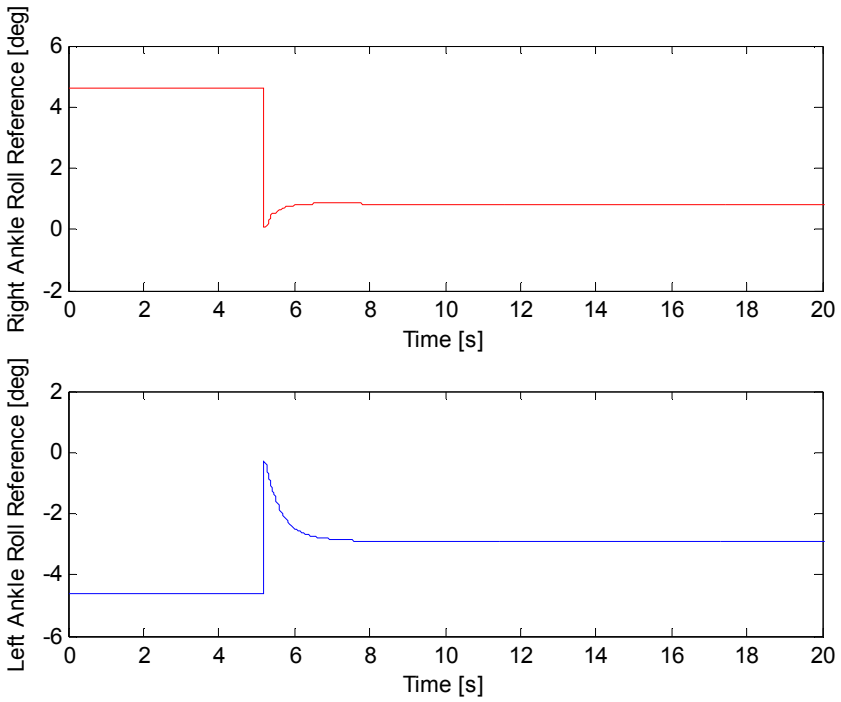

Figure 6.2 Roll angle references (Foot orientation control)

Pitch torque difference compensation modified the ankle pitch angles, so that both feet adapt to the ground conditions (Figure 6.3). It can be noted that the same torque difference is added to right and left ankles with opposite signs.

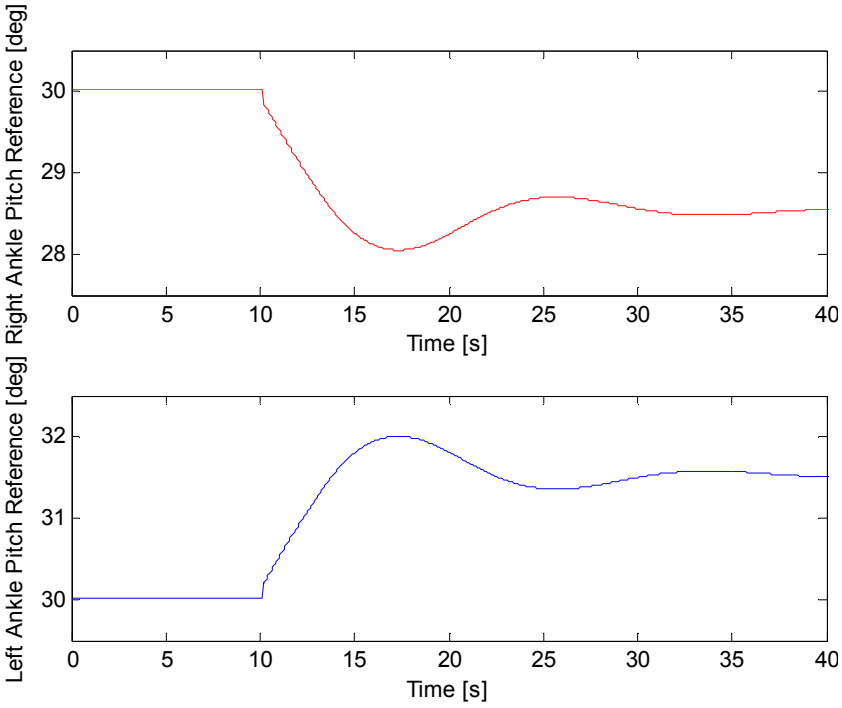

Figure 6.3 Pitch angle references (Pitch torque difference compensation)

In order to make the robot trunk straight, the trunk orientation control modified both ankle pitch angles and the effective lengths for both legs (Figure 6.4 and Figure 6.5). It can be seen that ankle pitch references start from the values after the pitch torque difference compensation and are now modified to the same direction to make the robot straight in pitch axis. Similarly, the effective lengths for right and left legs are altered to align the robot flat in roll axis. The trunk angles are shown in Figure 6.6.

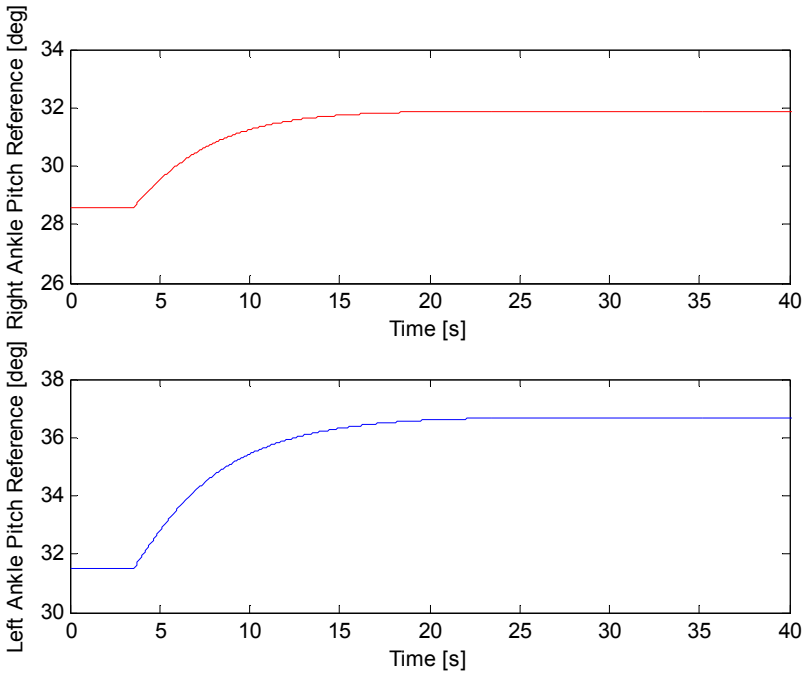

Figure 6.4 Pitch angle references (Trunk orientation control)

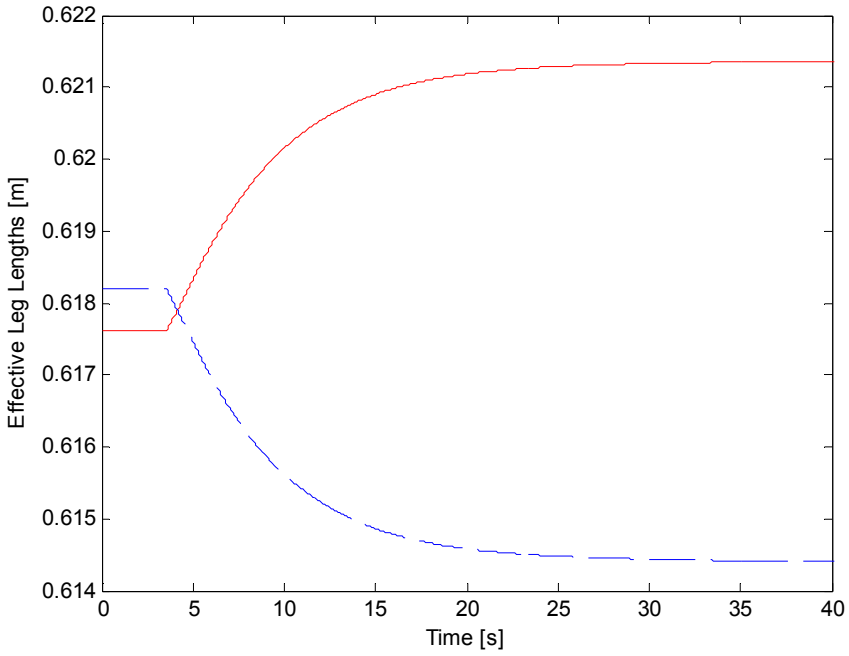

Figure 6.5 Effective length modifications for right (solid) and left (dashed) leg

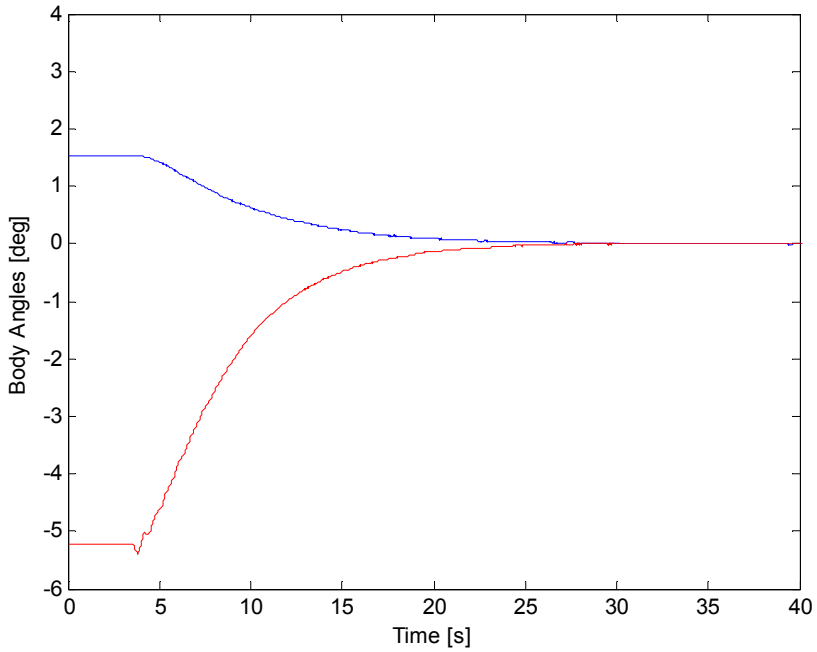

Figure 6.6 The roll (blue) and pitch (red) angle of the robot trunk

Since both legs are adapted to the ground in both roll and pitch axes and the trunk is in an upright position, the pitch torque at the ankles can be observed at the end of these three compensation algorithms (Figure 6.7). At the beginning of the homing process, the feet contact with different surfaces and the ankle pitch torques smoothly converge to the same steady state value after the automatic home posture adjustment.

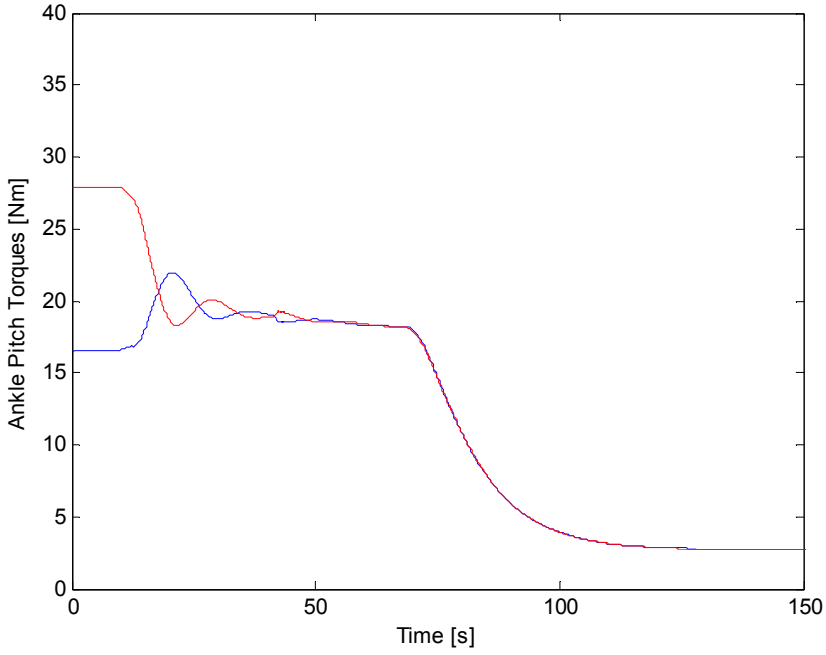

Figure 6.7 Pitch torques at the right (red) and left (blue) ankle

Finally, for even distribution of weight, $x_{ref\_asymmetry}$ and $y_{ref\_asymmetry}$ are modified such that the actual ZMP of the robot is on top of the desired ZMP value shown in Figure 5.2. The following figure plots the compensation of $x_{ref\_asymmetry}$ and $y_{ref\_asymmetry}$ values during the homing process.

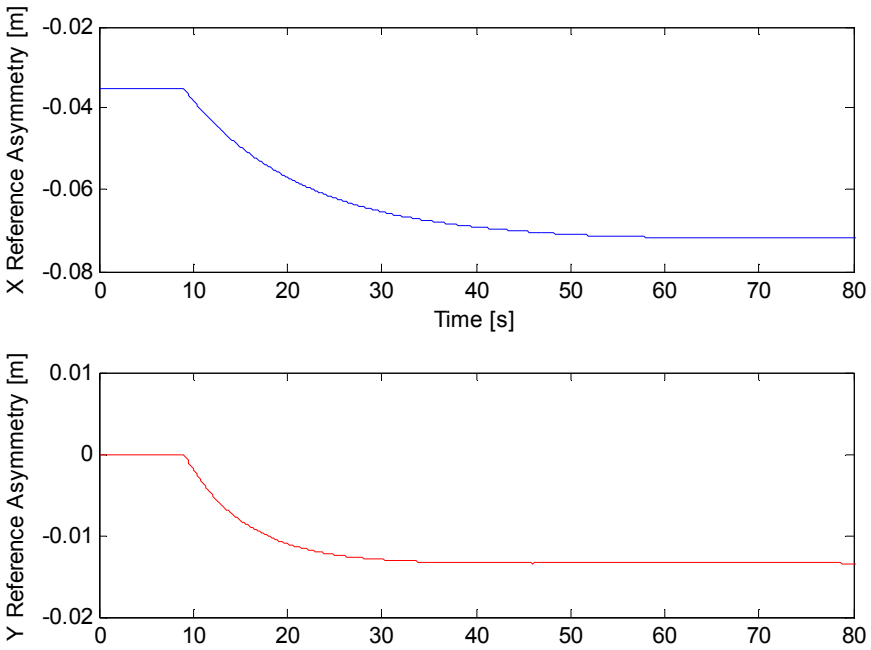

Figure 6.8 *x* and *y*-reference asymmetry modifications

6.2. Walking Results on Even Surface

The walking of SURALP is tested on a flat surface. Cartesian foot trajectories explained in Chapter 4 are generated and employing the control techniques discussed in Chapter 5, a stable walking is achieved. The following snapshots are taken during the walk of SURALP on an even terrain (Figure 6.9).

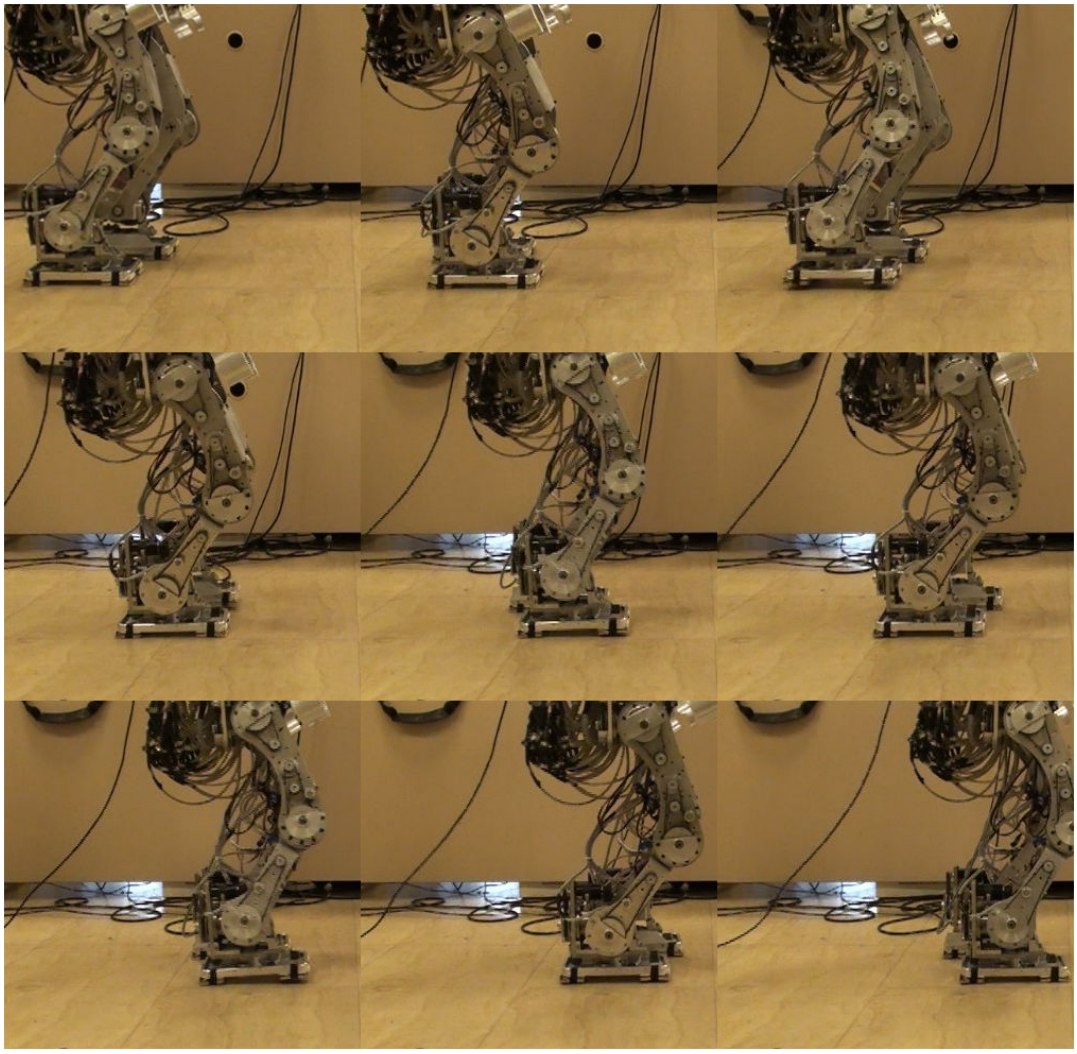

Figure 6.9 Snapshots of SURALP during the walk

In order to verify the effectiveness of the initial homing procedure, the body angles of the robot is captured and compared. It can be stated that the body roll and pitch angles are increased and the stability of the robot is weakened in terms of the repeatability of the oscillations (Figure 6.10). Better results are presented with the automatic homing procedure in the following figures.

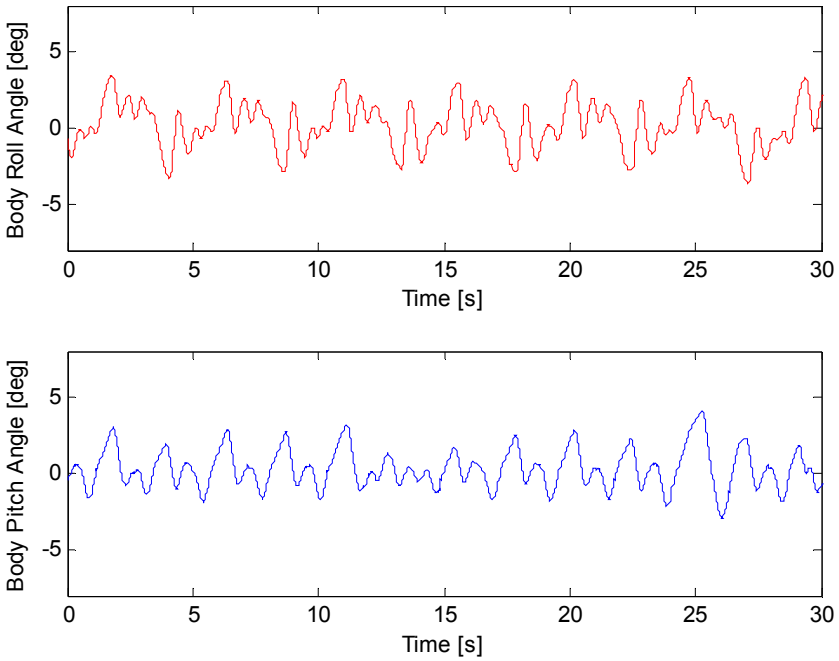

Figure 6.10 Body roll angles without automatic homing

After verifying the effectiveness of the homing procedure, the effects of the proposed control algorithms will be investigated. Figure 6.10 shows the ankle roll angle modification in the walking. The comparison of the original and the modified ankle roll angle references shows the effect of the foot orientation control. The foot orientation control modifies the ankle joint references to keep the feet parallel to the ground based on the torque feedback measured at the ankles.

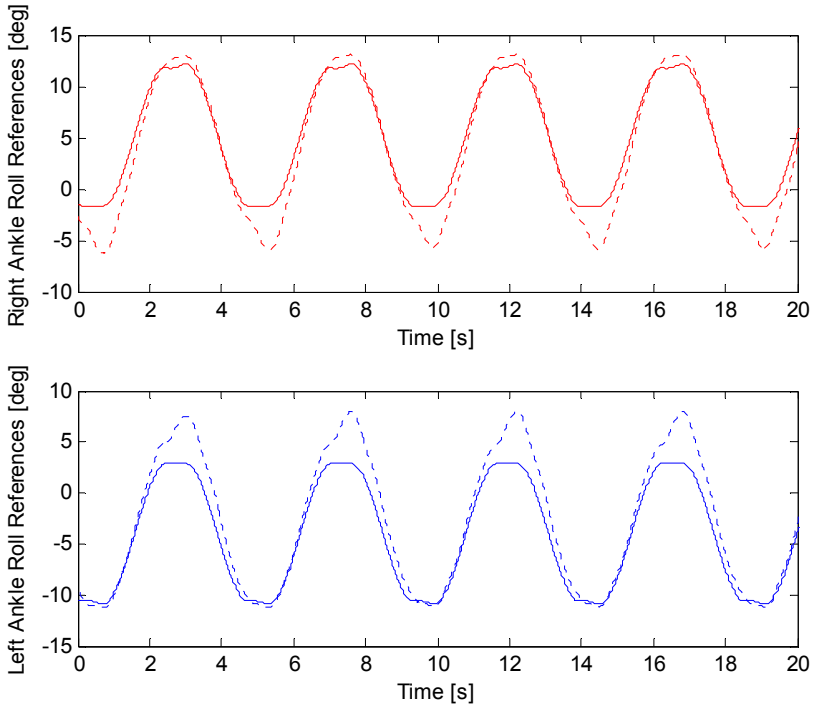

Figure 6.11 The roll angle reference of the ankles (original: solid, modified: dashed)

The advantage of this control method can be realized by observing the body roll angles and the roll torques at the feet. Figure 6.11 shows that the peaks of the regular body roll angle increased from [-3.5, 3.5] to [-4.5, 4.5], the robot started to oscillate in roll direction and lost balance at the end of the experiment. Figure 6.12 shows the significant increase in the oscillations of left ankle torque values around the roll axis, after the deactivation of the foot orientation control at t = 15 s.

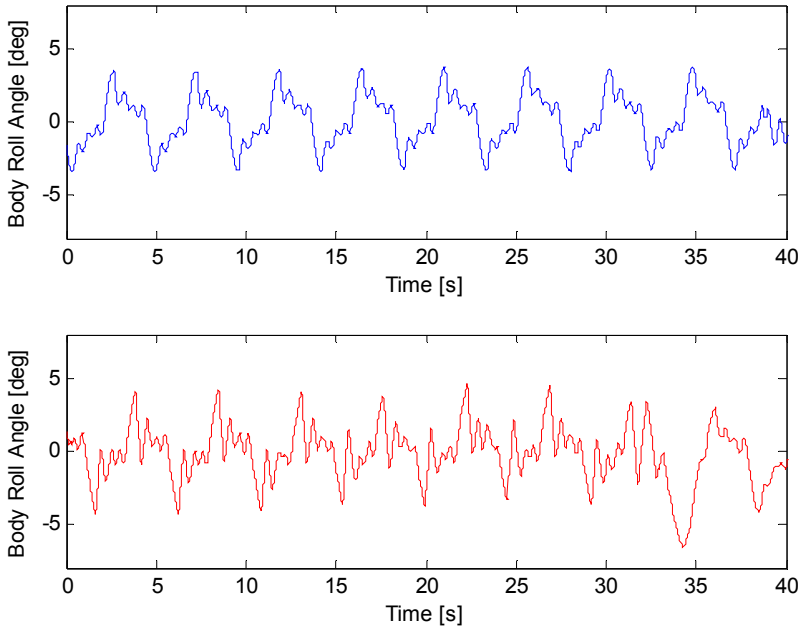

Figure 6.12 The roll angles of the robot body (with foot orientation control: top, without the control: bottom)

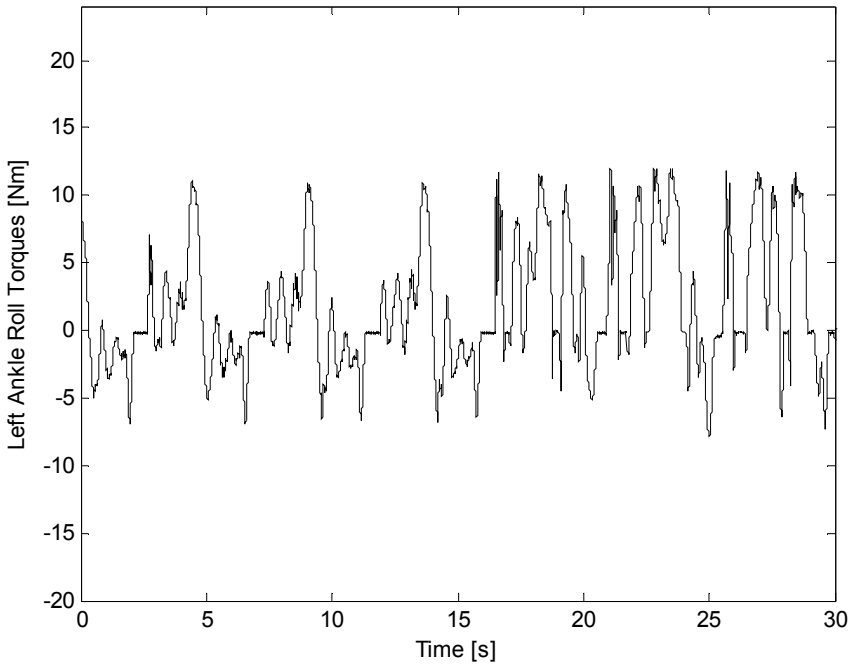

Figure 6.13 Left ankle roll torque values (foot orientation control deactivated at t=40 s.)

The modifications of the effective leg lengths by the ground impact compensation are shown in Figure 6.14. As explained in Chapter 5, using the measured ground interaction force on the landing foot, the impact is absorbed via a second order virtual mass-spring-damper system. After the activation time defined by the control designer, the modified distance returns to its original value by a smooth transition. The stability of the walk is verified by the smoothness and the repeatability of the modification of the effective leg lengths. The impact compensation is turned off at t = 25 and the robot started to tip over due to the impact forces at landing (Figure 6.15).

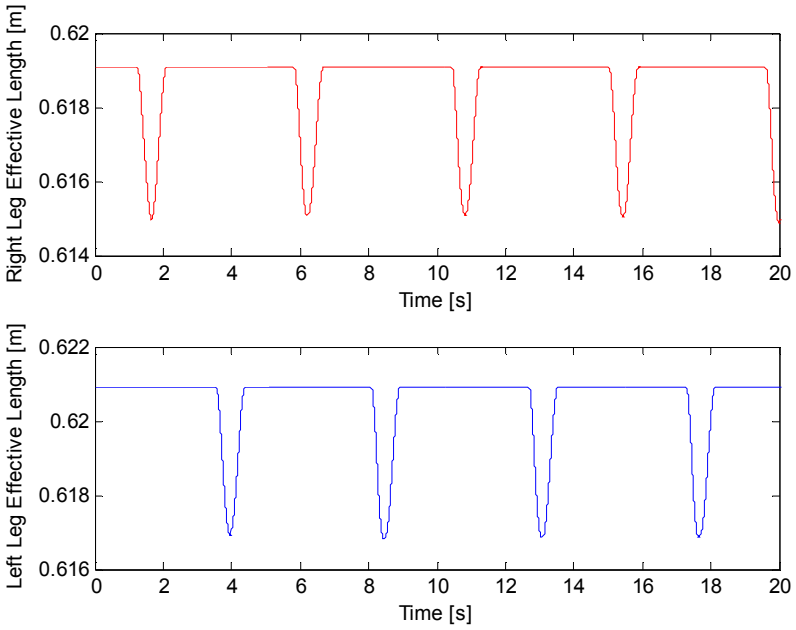

Figure 6.14 Effective leg length modifications

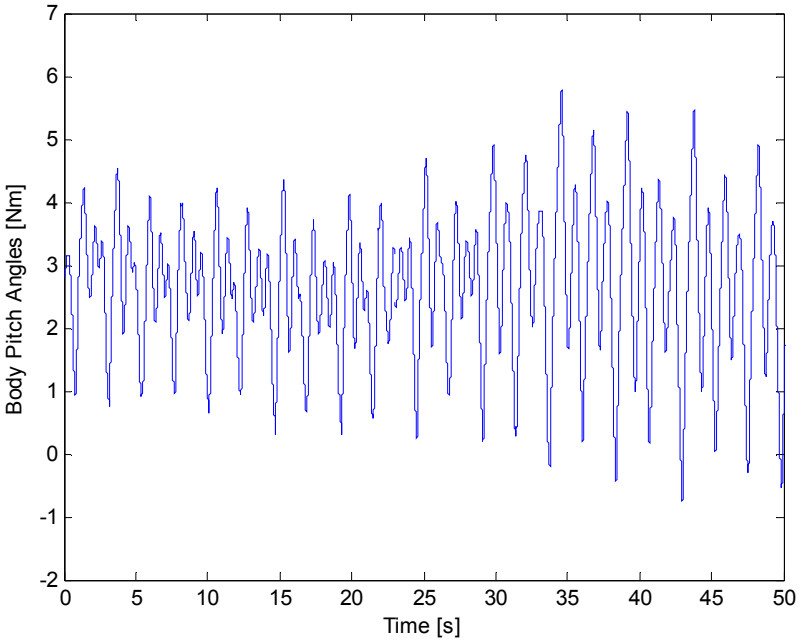

Figure 6.15 The body pitch angles (ground impact compensation turned off at t=25 s.)

As described in Section 5.3.3, early landing modification modifies the *x*-direction foot references in the case of an early landing, which is realized by the force/torque sensors at the ankles. The reference modifications for the left and right feet are shown in Figure 6.16.

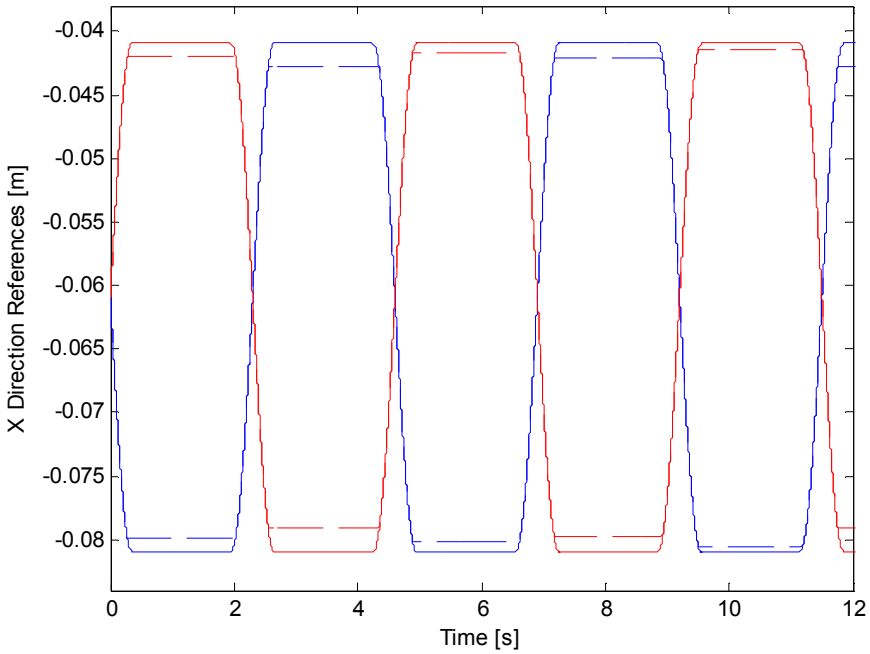

Figure 6.16 Early landing modifications (original: solid, modified: dashed) (right: red, left: blue)

As described in Section 5.3, the body pitch angle correction is activated to reduce the pitch angle oscillations during the walk. Figure 6.17 shows the control action of the proposed algorithm.

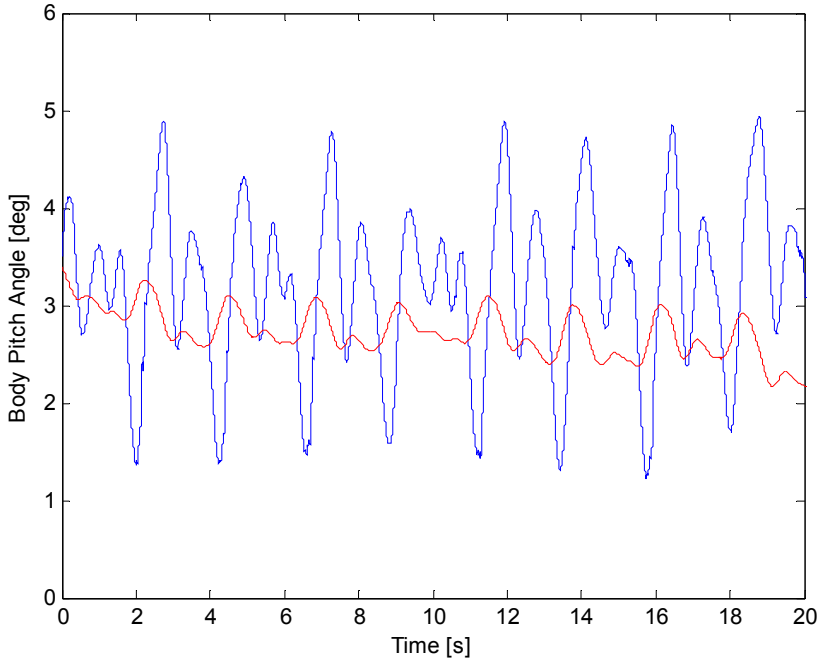

Figure 6.17 Body pitch angle correction effort (pitch angle: blue, control: red)

Employing this angle correction technique, the body pitch angle oscillations are reduced as shown in Figure 6.18. It is important to note that the control algorithm tries the body pitch angle to follow the pitch tilt angle reference, mentioned in 4.2.2.

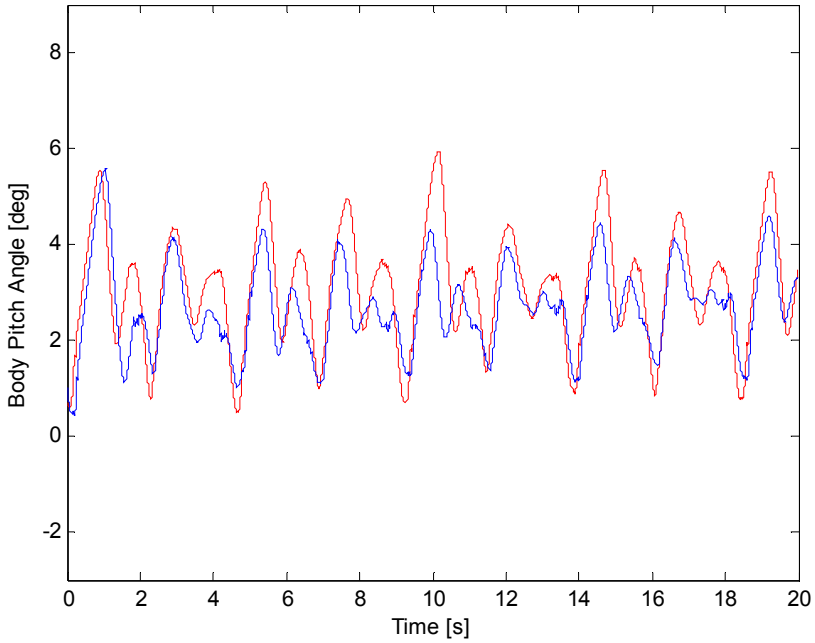

Figure 6.18 Body pitch angle correction (original: red, modified: blue)

Finally, the yaw moment values at the right ankle are investigated. With the help of the yaw moment compensation using waist and arm swing references, the magnitude of yaw moment oscillations are small enough to avoid the slipping of the feet and turning of the robot (Figure 6.19).

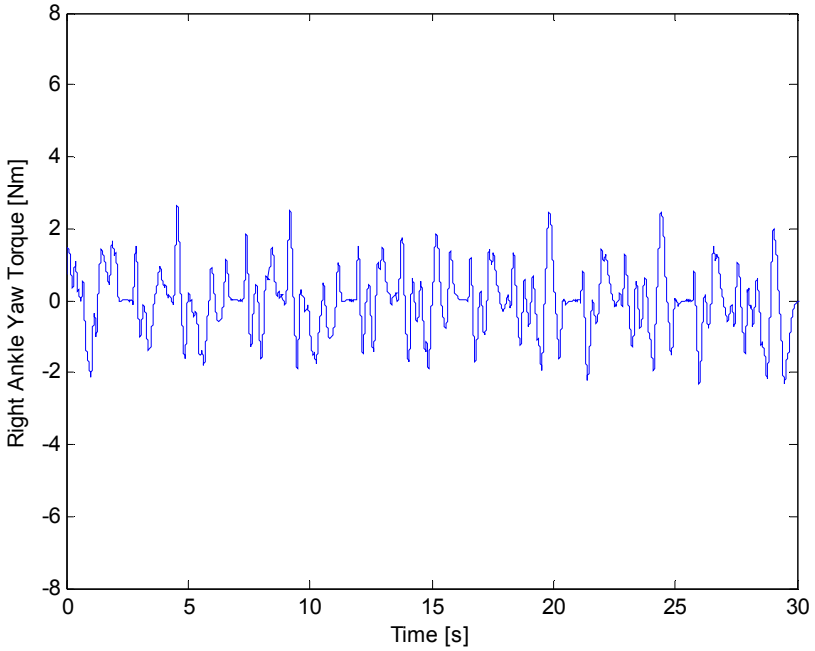

Figure 6.19 Right ankle yaw torque values

Chapter 7

7. CONCLUSION

A smooth trajectory generation and a number of online walking control algorithms are presented in this thesis.

The Cartesian foot reference trajectories are generated as periodic mathematical functions with respect to a coordinate frame attached to the trunk of the biped robot. The foot trajectories are smoothened at specific instants of the walk and the walking parameters are tuned online. Moreover, a ground push motion for the feet in the vertical direction is introduced.

For the realization of a dynamically stable walk, various walking control algorithms are presented using the sensory feedback from F/T sensors and the inclinometer. Furthermore, an automatic homing procedure is developed for the adjustment of the initial posture before the walking experiments.

The walking experiments on the humanoid robot platform SURALP verified the effectiveness of the proposed improvements on the trajectory generation and the p walking control algorithms. Successful experimental results on the robust walk of the robot are obtained.

Chapter 8

8. APPENDIX

A. Axis Assignment of the Legs of SURALP

The joint axis representation of the legs as explained in [51] is given as the following (Figure 8.1). The joint axes are assigned according to Denavit-Hartenberg methodology [47].

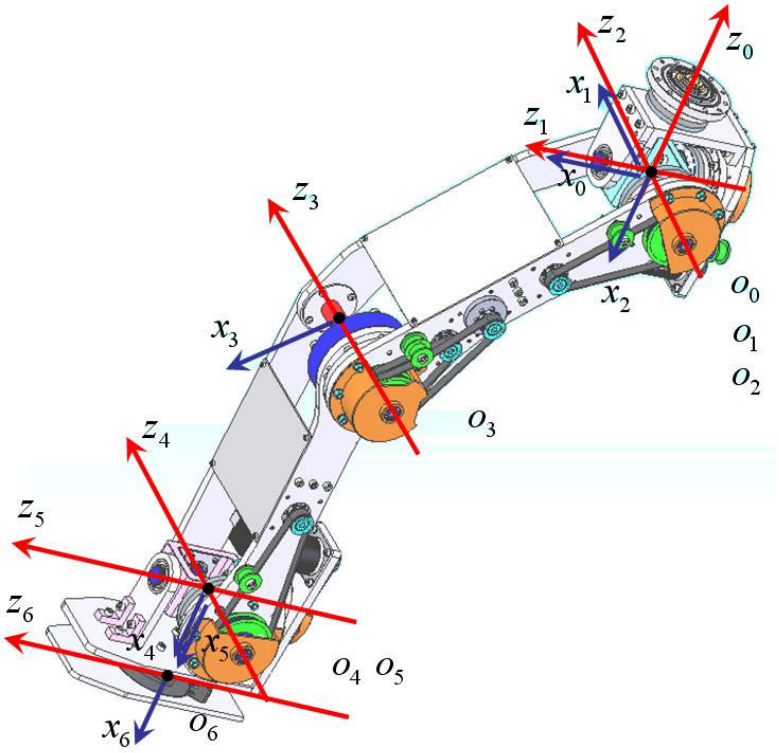

Figure 8.1 Denavit-Hartenberg joint axis representations for one leg

The Denavit Hartenberg parameters used in the computation of inverse kinematics are given in Table 8.1.

Table 8.1

Denavit-Hartenberg parameters of the biped leg

Link	a_i	α_i	d_i	θ_i
1	0	$\pi/2$	0	θ_1^*
2	0	$-\pi/2$	0	θ_2^*
3	L_3	$\pi/2$	0	θ_3^*
4	L_4	0	0	θ_4^*
5	0	$-\pi/2$	0	θ_5^*
6	L_6	0	0	θ_6^*

REFERENCES

[1] Takanishi, A., Lim, H., "Biped walking robots created at Waseda University: WL and Wabian family", *Philosophical Transactions of the Royal Society, Series A, 365 (1850), pp. 49-64,* 2007.

[2] Takanishi, A., Ishida, M., Yamazaki, Y., Kato, I., "The realization of dynamic walking by the biped walking robot WL-10RD", *Proceedings of International Conference on Advanced Robotics, pp. 459-466*, Tokyo, Japan, September 1985.

[3] Takanishi, A., Lim H., "Waseda Biped Humanoid Robots Realizing Human-like Motion", *Proceedings of the International Workshop on Advanced Motion Control, pp. 525-530,* Nagoya, Japan, March 2000.

[4] Nishiwaki, V., Sugihara, T., Kagami, S., Kanehiro, F., Inaba, M., Inoue, H., "Design and Development of Research Platform for Perception-Action Integration in Humanoid Robot: H6", *Proceedings of the 2000 IEEE/RSJ International Conference on Intelligent Robots and Systems, vol.3*, *pp. 1559-1564,* Takamatsu, Japan, October 2000.

[5] Nishiwaki, V., Kuffner, J., Kagami, S., Kanehiro, F., Inaba, M., Inoue, H., "The experimental humanoid robot H7: a research platform for autonomous behavior", *Philosophical Transactions of the Royal Society, Series A, 365 (1850), pp. 79-107,* 2007.

[6] Oh, J.-Y., Kim, J.-H., "Realization of dynamic walking for the humanoid robot platform KHR-1" *Advanced Robotics, vol. 18, no. 7, pp. 749-768,* 2004.

[7] Kim, J.-Y., Park, I.-W., Oh, J.-H., "Walking Control Algorithm of Biped Humanoid Robot on Uneven and Inclined Floor" *Journal of Intelligent and Robotic Systems, vol. 48, no. 4, pp. 457-484,* April 2007.

[8] Park, I.-W., Kim, J.-Y., Lee, J., Oh, J.-H., "Online Free Walking Trajectory Generation for Biped Humanoid Robot KHR-3 (KAIST Humanoid Robot-3: HUBO)" *2006 6th IEEE-RAS International Conference on Humanoid Robots, pp. 398-403,* Genova, Italy, December 2006.

[9] Gienger, M., Löffler, K., Pfeiffer, F., "Towards the design of a biped jogging robot", *Proceedings of the IEEE International Conference on Robotics and Automation, vol. 4, pp. 4140-4145*, Seoul, Korea, May 2001.

[10] Lohmeier, S., Buschmann, T., Ulbrich, H., Pfeiffer, F., "Modular joint design for performance enhanced humanoid robot LOLA", *Proceedings of the IEEE International Conference on Robotics and Automation, vol.4, pp. 88-93*, Orlando Florida, USA, May 2006.

[11] http://world.honda.com/ASIMO/

[12] Hirose, M., Ogawa, K., "Honda humanoid robots development", *Philosophical Transactions of the Royal Society, Series A, 365 (1850), pp. 11-19,* 2007.

[13] Hirose, M., Ogawa, K., "Walking biped humanoids that perform manual labour", *Philosophical Transactions of the Royal Society, Series A, 365 (1850), pp. 65-77,* 2007.

[14] Kaneko, K., Harada, K., Kanehiro, F., Miyamori, G., Akachi, K., "Humanoid Robot HRP-3" *Proceedings of 2008 IEEE/RSJ International Conference on Intelligent Robots and Systems, pp. 2471-2478,* Nice, France, September 2008

[15] Cheng, G., Hyon, S., Morimoto, J., Ude, A., Hale, J. G., Colvin, G., Scroggin, W., Jacobsen, S. C., "CB: A Humanoid Research Platform for Exploring NeuroScience," *Advanced Robotics, vol. 21, no. 10, pp. 1097–1114,* 2007.

[16] Ishida, T., Kuroki, Y., Yamaguchi, J., Fujita, M., Doi T., "Motion Entertainment by a Small Humanoid Robot Based on Open-R", *Proceedings of the IEEE International Conference Intelligent Robots and Systems, vol.2, pp. 1079-1086*, Maui, Hawaii, USA, October 2001.

[17] Kuroki, Y., Fujita, M., Ishida, T., Nagasaka, K., Yamaguchi, J., "A Small Biped Entertainment Robot Exploring Attractive Applications", *Proceedings of the IEEE International Conference on Robotics and Automation, vol.1, pp. 471-476,* Taipei, Taiwan, September 2003.

[18] http://pr.fujitsu.com/en/news/2001/09/10.html

[19] Yokoi, K., "Humanoid Robotics", *Proceedings of International Conference on Control, Automation and Systems,* Seoul, Korea, October 2007.

[20] http://en.wikipedia.org/wiki/Sagittal_plane

[21] Vukobratovic, M., Borovac, B., Surla, D., Stokic, "Biped Locomotion: Dynamics, Stability, Control and Application", Springer-Verlag, 1990.

[22] Huang, Q., Kaneko, K., Yokoi, K., Kajita, S., Kotoku, T., Koyachi, N., Arai, H., Inamura, N., Komoriya, K., Tanie, K., "Balance Control of a Biped Robot Combining Off-line Pattern with Real-time Modification", *Proceedings of the 2000 IEEE International Conference on Robotics & Automation, vol. 4, pp. 3346-3352,* San Francisco, CA, USA, April 2000.

[23] Kajita, S., Kanehiro, F., Kaneko, K., Yokoi, K., Hirukawa, H., "The 3D Linear Inverted Pendulum Mode: A simple modeling for a biped walking pattern generation" *Proceedings of the 2001 IEEE/RSJ International Conference on Intelligent Robots and Systems pp. 239-246,* Maui, Hawaii, USA, October 2001.

[24] Hirai, K., Hirose, M., Haikawa, Y. and Takenaka, T., "The Development of Honda Humanoid Robot", *Proceedings of the IEEE International Conference on Robotics and Automation, pp. 1321-1326, vol.2*, May 1998.

[25] Kajita, S., Espiau, B., "Legged Robots" *Springer Handbook of Robotics, Ch. 16, pp. 361-388.* Springer-Verlag, 2008.

[26] Gökçe, B., "Implementation Of Biped Walking Algorithm on Simulator and Humanoid Robot", Thesis (MS), Department of Computer Engineering of the Institute for Graduate Studies in Science and Engineering of Boğaziçi University, January 2009.

[27] Zheng, Y. F., "A Neural Gait Synthesizer for Autonomous Biped Robots", *Proceedings of the IEEE International Workshop on Intelligent Robots and Systems, vol. 2, pp. 601-608,* Ibaraki, Japan, July 1990.

[28] Walker, P., Grillner S., Buchanan, J.T., Brodin, L., "Neural control of locomotion in lower vertebrates" *Neural Control of Rhythmic Movements in Vertebrates, John Wiley & Sons, pp. 1-40*, 1988.

[29] Pinto, C.A., Golubitsky, M., "Central pattern generators for bipedal locomotion", *Journal of Mathematical Biology, vol. 53, pp. 474-489,* 2006.

[30] Righetti, L., Ijspeert, A.J., "Programmable Central Pattern Generators: an application to biped locomotion control" *Proceedings of the 2006 IEEE International Conference on Robotics and Automation, pp. 1585-1590,* May 2006.

[31] Kim J.-Y., Park I.-W., Oh J.-H., "Experimental Realization of dynamic walking of the biped humanoid robot KHR-2 using zero moment point feedback and inertial measurement", *Advanced Robotics, vol. 20, no. 6, pp. 707-736,* 2006.

[32] Nakajima, Y., Yonemura, A., Kawamura, A., "Experimental Approach for the Fast Walking by the Biped Robot", *Proceedings of the IASTED International Conference on Robotics and Applications,* Honolulu, Hawaii, USA, August 2000.

[33] Zhu, C., Okamura, M., Kawamura, A., Tomizawa, Y., "Experimental approach for high speed walking of the biped robot MARI-1", *Proceedings of the 8th IEEE International Workshop on Advanced Motion Control (AMC2004), pp. 427-432,* March 2004.

[34] El-Kahlout, Y., Erbatur, K., "Reflex and Gait Adaptation for Biped Walking Robots in Phase of Changing Payloads," *Proceedings of the International Conference on Industrial Electronics, Control and Instrumentation IECON 2003, pp. 484-489,* Virginia, USA

[35] Bebek, O., Erbatur, K., "A Fuzzy System for Gait Adaptation of Biped Walking Robots," *Proceedings of the IEEE Conference on Control Applications*, *CCA 2003, , pp. 669-673*, Istanbul, Turkey

[36] Takanishi, A., Takeya, T., Karaki, H., Kato, I., "A Control Method for Dynamic Biped Walking Under Unknown External Force", *Proceedings of the IEEE International Workshop on Intelligent Robots and Systems IROS'90, vol. 2, pp. 795-801,* Ibaraki, Japan, July 1990.

[37] Yamaguchi, J.-I., Takanishi, A., Kato, I., "Development of A Biped Walking Robot Compensating for Three Axis Moment by Trunk Motion", *Proceedings of the 1993 IEEE/RSJ International Conference on Intelligent Robots and Systems, vol.1, pp. 561-566,* Yokohama, Japan, July 1993.

[38] Takenaka, T., "The control system for the Honda humanoid robot", *Age and Ageing 2006, 35-S2, pp. 24-26.*

[39] Yokoi, K., Kanehiro, F., Kaneko, K., Fujiwara, K., Kajita, S., Hirukawa, H., "A Honda humanoid robot controlled by AIST software" *Proceedings of the IEEE-RAS International Conference on Humanoid Robots, pp. 259-264.*

[40] Nunez, V., Nadjar-Gauthier, N., Yokoi, K., Blazevic, P., Stasse, O., "Whole body posture controller based on inertial forces" *Proceedings of the 6th IEEE/RAS International Conference on Humanoid Robots, pp. 188-193,* December 2006.

[41] Kagami, S., Kanehiro, F., Tamiya, Y., Inaba, M., Inoue, H., "Autobalancer: An online dynamic balance compensation scheme for humanoid robots" *Proceedings of the Fourth International Workshop on Algorithmic Foundations on Robotics (WAFR'00), pp. 79-89,* 2000.

[42] Sugihara, T., Nakamura, Y., "Whole-body cooperative balancing of humanoid robot using COG Jacobian", *Proceedings of the 2002 IEEE/RSJ International Conference on Intelligent Robots and Systems, vol.3, pp. 2575-2580,* 2002.

[43] Kajita, S., Kanehiro, F., Kaneko, K., Fujiwara, K., Harada K., Yokoi K., Hirukawa, H., "Resolved momentum control: humanoid motion planning based on the linear and angular momentum" *Proceedings of the 2003 IEEE/RSJ International Conference on Intelligent Robots and Systems, vol.2, pp. 1644-1650,* October 2003.

[44] Pratt, J., Carff, J., Drakunov, S., Goswami, A., "Capture Point: A Step toward Humanoid Push Recovery", *Proceedings of the 6th IEEE/RAS International Conference on Humanoid Robots, pp. 200-207,* December 2006.

[45] Komura, T., Leung, H., Kudoh, S., Kuffner, J., "A Feedback Controller for Biped Humanoids that Can Counteract Large Perturbations During Gait" *Proceedings of the 2005 IEEE International Conference on Robotics and Automation, pp. 1989-1995,* Barcelona, Spain, April 2005.

[46] Erbatur, K., Seven, U., Taşkıran, E., Koca, Ö., Kızıltaş, G., Ünel, M., Sabanovic, A., Onat, A., "SURALP-L, The Leg Module of a New Humanoid Platform," *Proceedings of the IEEE/RAS International Conference on Humanoid Robots, pp. 168-173,* Daejeon, Korea, December 2008.

[47] Spong, M., Vidyasagar, M., "Robot Dynamics and Control", John Wiley and Sons, 1989.

[48] Erbatur, K., Seven, U., Taşkıran, E., Koca, Ö., Yılmaz, M., Kızıltaş, G., Ünel, M., Sabanovic, A., Onat, A., "SURALP: A New Full-Body Humanoid Robot Platform" accepted for publication in *Proceedings of the 2009 IEEE/RSJ International Conference on Intelligent Robots and Systems,* St. Louis, MO, USA, October 2009.

[49] Kim, J.-H., Kim, J-Y., Oh, J.-H., "Adjustment of home posture of a biped humanoid robot using an inertial sensor and force torque sensors" *Proceedings of the 2007 International Conference on Intelligent Robots and Systems (IROS'07), pp. 2223-2229,* October 2007.

[50] Koca, Ö., "ZMP Based Reference Generation for A Bipedal Humanoid Robot", Thesis (MS), Department of Mechatronics Engineering of the Graduate School of Engineering and Natural Sciences of Sabanci University, August 2009.

[51] Seven U., “Linear Inverted Pendulum Model and Swing Leg Dynamics in Biped Robot Walking Trajectory Generation”, Thesis (MS), Department of Mechatronics Engineering of the Graduate School of Engineering and Natural Sciences of Sabanci University, July 2007.